Universidade de Aveiro Departamento de Ciências Médicas

2017

Daniela Alexandra Costeira de Sousa

"Estimulação de uma linha celular de pDCs com imumocomplexos com o próprio DNA"

"Stimulation of a pDC cell line with self-DNA immune complexes"

Universidade de Aveiro Departamento de Ciências Médicas
2017

Daniela Alexandra Costeira de Sousa

"Estimulação de uma linha celular de pDCs com imumocomplexos com o próprio DNA"

"Stimulation of a pDC cell line with self-DNA immune complexes"

Tese apresentada à Universidade de Aveiro para cumprimento dos requisitos necessários à obtenção do grau de Mestre em Biomedicina Molecular, realizada sob a orientação científica da Doutora Catarina R. Almeida, Professora Auxiliar do Departamento de Ciências Médicas da Universidade de Aveiro

Apoio financeiro da FCT e do Portugal2020 (FEDER) através dos projetos UID/BIM/04501/2013 e PTDC/IMI-IMU/3615/2014.

o júri

presidente

Prof. Doutora Ana Gabriela da Silva Cavaleiro Henriques
professora auxiliar convidada da Universidade de Aveiro

Prof. Doutora Maria do Rosário Gonçalves dos Reis Marques Domingues
professora auxiliar convidada da Universidade de Aveiro

Prof. Doutora Catarina Rodrigues de Almeida
professora auxiliar convidada da Universidade de Aveiro

agradecimentos

A realização desta dissertação de mestrado contou com o importante apoio, incentivo e dedicação por parte de várias pessoas, às quais não posso deixar de exprimir a minha gratidão.

Aos Meus Colegas de Laboratório, Rita, Carolina e Paulo, por toda a ajuda e partilha de conhecimento para comigo.

À Professora Doutora Catarina Almeida, expresso o meu profundo agradecimento pela oportunidade de integrar no seu Grupo de Investigação, pelo seu profissionalismo e orientação que em muito acrescentou ao meu conhecimento científico, assim como à responsabilidade em mim incutida neste projeto.

Aos Meus Amigos, em especial à Leny, à Susana, à Valérie e à Liliana pelos intermináveis desabafos e amparo em momentos menos bons.

À Minha Família, em especial aos Meus Pais, ao Meu Irmão e aos Meus Avós, um enorme e sincero obrigada por acreditarem em mim, por todo o carinho, apoio e dedicação constante, e por terem sido um pilar e um porto de abrigo ao longo de todo este processo. A eles, dedico todo este trabalho.

palavras-chave

pDCs, linha celular CAL-1, immunocomplexos, DNA próprio, LL37, activação inata.

resumo

As células dendríticas plasmacitóides (pDCs) são um subtipo de Células Dendríticas que quando estimuladas podem produzir mediadores pro-inflamatórios e IFNs do tipo I. Estas células desempenham um papel importante em doenças autoimunes como o lúpus sistémico eritematoso, uma vez que podem ser ativadas por imunocomplexos formados por DNA do próprio, que desencadeia uma resposta de IFNs do tipo I através da via de sinalização do TLR-9. Aqui, otimizamos a ativação das células CAL-1, uma linha celular de pDCs, com imunocomplexos de DNA nuclear ou mitocondrial do próprio com o péptido antimicrobiano LL37, em paralelo com a estimulação com CpG-A. Descobrimos que elevadas concentrações de LL37 reduzem a viabilidade celular das CAL-1. O próprio DNA-LL37 despoletam a expressão de IFN-α e IFN-β nas células CAL-1, sem induzir a expressão de TNF-α, tal como em pDCs primárias. As concentrações ideais de DNA e LL37 nos complexos que levam a uma forte ativação das CAL-1 são 0.2μg/ml e 10μg/ml, respetivamente. Também descobrimos que as células CAL-1 estimuladas com imunocomplexos de DNA nuclear do próprio, mas não de DNA mitocondrial do próprio, foram capazes de secretar a citocina pro-inflamatória IL-1β. A análise imunocitoquímica revelou que os endossomas iniciais e o TLR-9 são recrutados após ativação por 30-60minutos com imunocomplexos. Assim, este trabalho estabele as células CAL-1 como um modelo celular para a ativação de com imunocomplexos.

keywords pDCs, CAL-1 cell line, immune complexes, self-DNA, innate activation.

abstract Plasmacytoid dendritic cells (pDCs) are a subset of Dendritic Cells that when stimulated can produce pro-inflammatory mediators and type I IFNs. These cells play an important role in autoimmune disease such as systemic lupus erythematosus, as they can become activated by immune complexes formed with self-DNA, which trigger a type I IFN response through the TLR-9 signaling pathway. Here, we optimized activation of CAL-1 cells, a human pDC cell line, with immunocomplexes of self-nuclear or mitochondrial DNA with the antimicrobial peptide LL37. It was found that high concentrations of LL37 led to a reduced CAL-1 cell viability. Self-DNA-LL37 triggered expression of IFN-α and IFN-β in CAL-1 cells, without inducing expression of TNF-α, as in primary pDCs. The concentrations of DNA and LL37 in the complexes leading to a stronger CAL-1 activation were 0.2μg/ml and 10μg/ml, respectively. We also found that CAL-1 cells stimulated with immune complexes with self-nuclear DNA, but not self-mitochondrial DNA, were capable of secreting the pro-inflammatory cytokine IL-1β. Immunocytochemistry analysis revealed that early endosomes and TLR-9 were recruited 30-60 minutes upon activation with immune complexes. Thus, this work established CAL-1 cells as a cell model for pDC activation with immune complexes.

Contents

List of Figures i
List of Abbreviations iii
List of Tables vii
I. Introduction 1
Diseases and Auto-immunity 4
Cytokines produced by pDCs 6
DC Activation 8
Activation by self-DNA immune complexes 12
CAL-1 cell line 16
Objectives 17
II. Materials & Methods 19
Cell culture 20
Preparation of DNA-complexes 20
Cell stimulation 22
Measuring RNA levels by qPCR 23
Measuring cytokine secretion by ELISA 26
Analysis of complex recognition by Immunofluorescence 27
Statistical Analysis 29
III. Results & Discussion 31
Serum batch choice 32
Optimizing LL37 Concentration for CAL-1 stimulation with immune complexes 36
Optimizing DNA Concentration for CAL-1 stimulation with immune complexes 42
Co-localization Analysis by IF 49
IV. Conclusions 55
V. Bibliography 57

List of Figures

Figure 1 - Cytokine production upon TLR-7/9 induction of MYD88–IRF7 and MYD88–NF-κB pathways.. 11

Figure 2- Growth curve for cells grown in medium supplemented with different sera. Live cells were counted after diluting in trypan blue for each time point indicated..... 32

Figure 3 – Flow Cytometry analysis of cell viability for CAL-1 cells. A –selection of the area containing events considered for analysis of cell viability (gating – P1 region); B – viable cells will not stain for propidium iodide and thus are located in the gated area (R1). 33

Figure 4 – Expression of mRNA for IFN-α (A), IFN-β (B) and TNF-α (C) was determined by RT-qPCR for CAL-1 cells cultured in medium supplemented with different batches of serum and stimulated with CpG-A. GAPDH was used as a reference gene and mRNA expression was normalized against values obtained for 0 h of incubation. 35

Figure 5 – Evaluation by Flow Cytometry of CAL-1 cells viability after 6h of stimulation with IC with different concentrations of LL37. Plots show the intensity of Propidium iodide staining (FL2) against FCS. The percentage of events (R6) represents the viable cells. A – cells with no treatment; B – cells treated with IC prepared with 5μg/ml of LL37; C – cells treated with IC prepared with 10μg/ml of LL37; D – cells treated with IC prepared with 20μg/ml of LL37; E – cells treated with IC prepared with 50μg/ml of LL37. 36

Figure 6 – Percentage of viable cells after 6h (A) and 24h (B) of incubation with immune complexes prepared with different LL37 concentrations (5, 10, 20 and 50μg/ml). Data was obtained by Flow Cytometry upon Propidium Iodide staining. 37

Figure 7 – Expression of mRNA for IFN-α (A), IFN-β (B) and TNF-α (C) was determined by RT-qPCR for CAL-1 cells incubated with immune complexes prepared with different LL37 concentrations (5, 10, 20 and 50μg/ml) and stimulated in parallel with CpG-A or with self-DNA, as controls. GAPDH was used as a reference gene and mRNA expression was normalized against values obtained for 0 h of incubation. Data are mean of four independent experiments, error bars represent the SEM..... 40

Figure 8 – Protein secretion determined by ELISA for CAL-1 cells incubated with immune complexes prepared with different LL37 concentrations (5, 10, 20 and 50μg/ml) and stimulated in parallel with CpG-A and only with self-DNA. A – IL-1β secretion; B – IFN-α secretion; C - TNF-α secretion Data are mean of five independent experiments, error bars represent the SEM. 41

Figure 9 - Expression of mRNA for IFN-α (A), IFN-β (B) and TNF-α (C) was determined by RT-qPCR for CAL-1 cells incubated with immune complexes prepared with different nDNA concentrations (1, 0.5 and 0.2μg/ml) and stimulated in parallel with CpG-A and only with LL37 and self-DNA. GAPDH was used as a reference gene and mRNA expression was normalized against values obtained for 0 h of incubation. Data are mean of four independent experiments, error bars represent the SEM..... 45

Figure 10 - Expression of mRNA for IFN-α (A), IFN-β (B) and TNF-α (C) was determined by RT-qPCR for CAL-1 cells incubated with immune complexes prepared with a concentration of 0.5μg/ml of mtDNA and stimulated in parallel with CpG-A and only with LL37 and self-mtDNA 47

Figure 11 - Secretion of IL-1β determined by ELISA for CAL-1 cells incubated for 6h (A) and 24h (B) with immune complexes prepared with different nDNA concentrations (1, 0.5, 0.2μg/ml) and mtDNA (0.5μg/ml) or stimulated in parallel with CpG-A or only with LL37 and self-DNA, self-mtDNA. 48

List of Abbreviations

AF	Alexa Fluor
AIM2	Absent in melanoma 2
AMP	Adenosine monophosphate
ANOVA	Analysis of variance
AP3	Adaptor protein 3
APC	Antigen presenting cell
BAD-LAMP	Brain and dendritic cell-associated lysosome-associated membrane protein
BDCA	Blood dendritic cell antigen
BSA	Bovine serum albumin
CCL	C-C motif chemokine ligand
CCR	C-C motif chemokine receptor
CD	Cluster of differentiation
cDC	Common dendrictic cell
cDNA	Complementary DNA
CpG	Cytosine triphosphate deoxynucleotide —phosphate—Guanine triphosphate deoxynucleotide
CXCL	C-X-C motif chemokine ligand
CXCR	C-X-C chemokine receptor
DAPI	4',6-Diamidino-2-Phenylindole
DC	Dendritic cell
DHX36	DEAH box protein 36
DNA	Deoxyribonucleic acid
DNase	Deoxyribonuclease
dNTP	Deoxynucleotide

dsDNA	double-stranded deoxyribonucleic acid
EEA1	Early endosome antigen 1
EGTA	Ethylene glycol-bis(β-aminoethyl ether)-N,N,N',N'-tetraacetic acid
ELISA	Enzyme-linked immunosorbent assay
ER	Endoplasmic reticulum
FBS	Fetal bovine serum
FCγR	Fc-gamma receptor
GAPDH	Glyceraldehyde 3-phosphate dehydrogenase
GM-CSF	Granulocyte-macrophage colony-stimulating factor
hCAP-18	Human cationic antimicrobial protein
HCl	Hydrogen chloride
HDP	Host-defense peptide
HEPES	4-(2-hydroxyethyl)-1-piperazineethanesulfonic acid
HEV	High endothelial venule
HLA-DR	Human leukocyte antigen D related
HMGB-1	High-mobility group box 1
HRP	Horseradish peroxidase
IC	Immune complex
IFN	Interferon
IFNAR	Interferon-α/β receptor
Ig	Immunoglobulin
IKK	I kappa B kinase
IL	Interleukin
ILT	Ig-like transcript
IPC	Interferon producing cell
IRAK	Interleukin-1 receptor-associated kinase

IRF	Interferon regulatory factor
LAMP	Lysosome-associated membrane protein
LAP	LC3-associated phagocytosis
LC3	Microtubule-associated protein 1A/1B-light chain 3
MAPK	Mitogen-activated protein kinase
MDA-5	Melanoma differentiation-associated protein
mDC	Myeloid dendritic cell
MHC	Major histocompatibility complex
mRNA	Messenger RNA
mtDNA	Mitochondrial DNA
MyD88	Myeloid differentiation primary response 88
NADPH	Nicotinamide adenine dinucleotide phosphate (reduced form of $NADP^+$)
nDNA	Nuclear DNA
NEAA	Non-essential amino acid
NET	Neutrophils release extracellular traps
NF-κB	Nuclear factor kappa B
NK	Natural-killer
NLR	Nod-like receptors
ODN	Oligodeoxyribonucleotide
OPN	Osteopontin
ORN	Oligoribonucleotide
Ox-mtDNA	Oxidized mtDNA
PAMP	Pathogen-associated molecular pattern
PBS	Phosphate buffered saline
pDC	Plasmacytoid dendritic cell

PFA	Paraformaldehyde
PI	Propidium Iodide
RAGE	Receptor for advanced glycation endproducts
RIG-I	Retinoic acid-inducible gene I
RNA	Ribonucleic acid
RNase	Ribonuclease
RPMI	Roswell Park Memorial Institute
RT	Room temperature
RT-qPCR	Real-time polymerase chain reaction
Siglec-H	Sialic acid binding Ig-like lectin H
SLE	Systemic lupus erythematosus
ssDNA	single-stranded deoxyribonucleic acid;
Th	T helper cell
TIR	Toll/IL-1 receptor
TLR	Toll-like receptor
TMB	Tetramethylbenzidine
TNF	Tumor necrosis factor
TRAF	TNF receptor associated factor
UNC93B	Protein UNC93 homolog B1
WHO	World health organization

List of Tables

Table 1 – Primer sequences for each target gene. 25

Table 2 - Concentration range for antibody concentration test. 28

Table 3- Antibody concentration for evaluation of TLR-9 and EEA1 recruitment of immunocomplexes with endosomal internalization..... 29

Table 4- Number of cells after culture in medium with 10% sera from different suppliers, at different time-points (0h, 24h, 48h, 72h and 96h).. 32

Table 5 - Percentage of viable cells for each serum and in each time point 33

Table 6 - Relative amount of IFN-α, IFN-β and TNF-α mRNA expressed by CAL-1 stimulated with the complexes formed with the indicated amount of LL37, measured by RT-qPCR, after 6h of incubation. 38

Table 7 - Relative amount of IFN-α, IFN-β and TNF-α mRNA expressed by CAL-1 stimulated with the complexes formed with the indicated amount of nDNA, measured by RT-qPCR, after 6h of incubation. 42

Table 8 – Relative amount of IFN-α, IFN-β and TNF-α mRNA expressed by CAL-1 stimulated with the complexes formed with the indicated amount of mtDNA, measured by RT-qPCR, after 6h of incubation. 46

I. Introduction

Plasmacytoid dendritic cells (pDCs) are a subpopulation of dendritic cells (DCs) specialized in secretion of type I interferons (IFNs) in response to viruses (1,2). DCs efficiently link the innate and the adaptive immune responses (3,4) via cytokine production and antigen presentation, being sentinels within the body. As a DC derived population, the cytokines produced by pDCs include type I IFNs, interleukine (IL)-6 and Tumor Necrosis Factor (TNF)-α (5,6). Activated pDCs also function as antigen presenting cells (APC) and have the potential to prime and promote differentiation of T cells into regulatory or inflammatory effector cells. For that, they survey tissues to capture and present antigens to instruct and shape the adaptive immune response either to respond or to be tolerant against peripheral antigen (4,7). These cells have immunoregulatory effects that are independent of type I IFN production, since they express Major Histocompatibility Complex (MHC) class II and co-stimulatory molecules such as CD40, CD86 (7) and CD80, being able to present antigens (4,8). After exposure to maturation stimuli such as Toll-like receptor (TLR) ligands, pDCs can prime $CD8^+$ T cells and $CD4^+$ T cells (4,7–9). However, they appear to be much less potent APCs compared to conventional DCs (cDCs) in stimulating T cells (4,8). pDCs do not always stimulate naive T cells but they can be converted into cDC-like cells upon activation and function as APCs (10), sometimes leading to tolerance induction by acting as immunogenic cells (11). More, type I IFN can regulate the function of B, T, DC and natural killer (NK) cells and can also alter the residence time of leukocytes within lymph nodes (2,4,12).

pDCs were first described in 1958 and mentioned as plasmacytoid monocytes or plasmacytoid T cells (13). Nowadays, pDCs are recognized as a DC subset family that develops from hematopoietic stem cells in bone marrow (6,14), being relatively abundant (1-2%) (15,16). They can also be found in peripheral blood in about 0.2% to 0.8%, in healthy individuals (17–19). Despite being a DC family, pDCs and cDCs share some similarities, but can be very different as well. DCs leave the bone marrow to give rise to resident and migratory DCs (20,21). Unlike cDCs, following their development in bone marrow, pDCs circulate through the bloodstream and reach T cell areas of the lymph nodes mainly through high endothelial venules (HEVs), entering to lymph nodes directly from the blood. Thus, under steady state conditions, pDCs are found in thymus, in secondary lymphoid tissues, and in rare numbers in peripheral tissues (2,4,8,20). On their surface, resident pDCs express low levels of chemotactic molecules such as CXCR4 that limits their motility, being required for their retention in the bone marrow stromal niche and for their development (8,20,22). Upon retention, pDCs are difficult to found in peripheral tissues such as skin and mucosa, however, high numbers have been found in injured tissues of autoimmune patients (19).

On the surface, pDCs express markers and receptors, that distinguish them from cDCs and regulates their functions (20). They were first identified in humans as CD4+, CD68+ and IL-3R+ (IL-3 receptor also known as CD123) plasma-like cells (23,24). It is now known that pDC lack expression of the lineage-associated markers CD3, CD19, CD14, CD16 and the DC marker CD11c. pDCs can be distinguished from other blood cells, by their expression of C-type lectin BDCA-2 (25), BDCA-4, B220 (4), and the immunoglobulin superfamily receptor immunoglobulin-like transcript 7 (ILT7) (26). They also express MHC-II, CD2 (11) and ILT3 (8). pDCs also show distinct molecular and cellular features that underlie their unique IFN-producing capacity. These include: prolonged endosomal retention of (TLRs) ligands, basal expression of interferon response factor 7 (IRF7) (the master regulator of IFN response), "plasmacytoid" secretory morphology, resembling antibody-secreting plasma cells, and expression of specific surface receptors that modulate IFN secretion, such as human ILT7 and BDCA-2, and Siglec-H in mouse (15,27,28).

pDCs show heterogeneous expression of several genes, suggesting a certain degree of developmental and/or functional heterogeneity (15). Thus, pDCs may not represent a homogenous population, but rather subpopulations with distinct functions (4). Accordingly, CD2 distinguishes two human pDC subsets, where $CD2^{hi}$ pDCs expresses lysozyme and displays cytolytic capacity, while $CD2^{low}$ do not (29). More, blood-derived pDCs can be subdivided into two different subsets - pDC1 and pDC2. These subsets differ in their phenotype and in their capacity to induce pro-inflammatory or regulatory T cell responses. pDC1 exhibit a more immature phenotype with low expression of MHC-II and null expression of the co-stimulatory molecule CD86, while pDC2 have a more mature phenotype, expressing MCH-II and CD86 (4). In 2011, a new pDC marker called BAD-LAMP (brain and DC associated LAMP-like molecule) was discovered. LAMP family members, specifically accumulate late endosomes and in lysosomes. In humans, is found in $CD123^{+}$BDCA-2^{+}BDCA-4^{+} pDCs and is mostly localized in the ER-Golgi intermediate compartment and does not display any obvious endosomal localization (30).

Recent studies suggested a new DC phenotypical evaluation. Six DC clusters numbered DC1 to DC6 were defined by single-cell RNA sequencing, where cluster DC6 is related to pDCs and cluster DC5 describes a new DC subset, named AS DCs. AS DCs seem to share gene expression signatures with cDCs and pDCs, but they activate T cells more efficiently than pDCs and are functionally different from pDCs. For example, pDCs (but not AS DCs) expressed genes associated with pathogen sensing and induction of type I IFN, like IRF7. Thus, "purified" pDCs were reclassified as the initially described "natural interferon producing cells (IPCs)" with lower capacity to induce T cell proliferation. AS DCs

were found to be identical to $CD2^{hi}$ pDC phenotype. AS DCs were also found morphological different from pDCs (31).

Diseases and Auto-immunity

pDCs are involved in several immune diseases. In normal conditions, self-nucleic acids are rapidly degraded in the extracellular environment and fail to access endosomal compartments spontaneously (32). However, self-DNA and self-RNA can trigger pDC activation when aberrantly transported into TLR-containing endosomes. That being the case, pDCs are continuously activated to produce type I IFNs, which drives disease onset (33,34).

Type I IFN production by pDCs in response to acute viral infections is usually limited in time and amplitude, becoming less important later in infection (35). The impact of pDCs depends on the route of infection, and the requirement of pDCs for antiviral defense during local infections only exists if other defense mechanisms are broken (36). However, chronic pDC activation can be seen in the absence of infection and may result in autoimmune diseases. In those cases, pDCs can sense self-DNA released from dying cells or in neutrophil extracellular traps complexed to an antimicrobial peptide LL37 in autoimmune diseases (37). Here, pDCs have been implicated in pathologies characterized by a type I IFN signature, such as systemic lupus erythematosus (SLE), atherosclerosis, and psoriasis (6,8,15,20). Despite the pathological role of pDCs in autoimmune skin diseases, the physiological importance of pDCs in initiating skin wound healing is also reported. Following skin injury, pDC are recruited to the site of tissue damage to sense self-nucleic acids released by dying cells in combination with cathelicidins, and to initiate tissue repair via TLR-induced IFN-α production (38).

SLE is the second most common autoimmune disease characterized by breakdown of tolerance to nuclear antigens and immunocomplexes (IC) deposition in tissues (39). Those complexes contain autoantibodies to nuclear 'autoantigens', nucleic acid and associated proteins, being formed in circulation and then deposited in tissues causing inflammation (40,41). SLE involves multiple organs, such as skin and blood vessels (39). Patients have reduced numbers of circulating pDCs, but high number in skin lesions, since upon activation pDCs upregulate expression of chemokine

receptors CXCR3 and CCR7, which traffic cells to peripheral sites of inflammation and the lymph nodes, respectively. The hallmark of SLE is the increased level of antinuclear antibodies present in 99% of individuals (33). SLE patients have also deficient B and T cell regulation, increased amounts of circulating cell material and cytokines at serum, that contribute to the inflammation. Furthermore, increased IFN-α levels at the serum are correlated to disease activity and severity (40). pDCs infiltrate the skin and show increased serum levels of IFN-α/β (42) upon delivery of immune complexes to endosomal compartments via the Fc receptor FcγRII, which promote activation of TLR-9 (17). IFN induction (43) can be enhanced by the association of HMGB1, DNA (41) and neutrophils release extracellular traps (NETs) containing chromatin DNA, and LL37 (39,44). Nucleic acids that stimulate pDCs in SLE may also be derived from other types of cellular death, such as necroptosis or pyroptosis, as well as from NADPH independent release of mitochondrial DNA (45).

Psoriasis is another chronic inflammatory skin disease that occurs in individuals with genetic predisposition and affects 2-3% of the population (46). The main feature of psoriasis is the abnormal activation of DC subsets in dermal compartments, leading to the downstream T-cell-mediated autoimmune cascade and the excessive production of AMPs and proteins by keratinocytes (47). pDCs appears to have a central role in this process since are present in lesional skin as the result of inflammatory process and associated cell damage (34,48). Then, engagement of TLR-9, leads to chronic IFN-α production by pDCs, activating myeloid DCs (37,48). Subsequently, T cells infiltrate the skin and secrete IFN-γ and Th17, initiating an abnormal and typical keratinocyte proliferation and epidermal differentiation (49).

Finally, atherosclerosis is a chronic cardiovascular pathology (20), being caused by a chronic inflammatory disease of the arterial wall, modulated by innate and adaptive immune responses (37). In this disease, monocytes acquire a phenotype that is consistent with inflammatory macrophages (50). Besides monocytes, macrophages and T cells, also pDCs can be detected within human atherosclerotic lesions (51). pDCs were found to co-localize with T cells in atherosclerotic plaques, supporting the atherosclerosis progression by production of IFN-α (20). pDCs activation also promotes unspecific amplification of humoral immune responses to antigens in atherosclerosis, specifically by production of dsDNA antibodies in early atherosclerosis. IFN-α expression prime reciprocally NETs release from neutrophils, driving positive feedback and amplification, supporting humoral immunity (52). Due to the NETs amplification (53), triggering production of IFN-α production through TLR-9-mediated signaling, by pDCs stimulated with selft-DNA-LL37 complexes (48). This shows that pDCs are not only present in lymph nodes and spleen but could also be detected

in atherosclerotic lesions, and it seems to correlate with plaque progression in human atherosclerosis (37).

mtDNA can be also involved in atherosclerosis by neutrophils release of mtDNA–protein complexes spontaneously in the absence of cell death and membrane disruption (54). LL37 is present in neutrophils and NETs in atherosclerotic lesions and, both nDNA and mtDNA are too, allowing the assembly of either LL37-nDNA and/or LL37-mtDNA complexes (53).

However, further studies are needed to understand these diseases and a cell line model of pDCs will greatly facilitate those studies.

Cytokines produced by pDCs

Upon activation, pDCs secrete high amounts of cytokines, such as IFN-α and IFN-β (55), inducing innate immunity initiation. Cells of the innate immune system sense common pathogen-associated molecular patterns (PAMPs), characteristic of pathogens, directly attack invading microbes and directing the adaptive immune system to mount a more precise response (56). IFNs are a family of cytokines that exhibit a broad range of properties beyond antiviral action (57) and are classified into 3 types, type I (including IFN-αs, -β, -ω, -ε) (58), type II (IFN-γ) (59) and type III (IFN-λ1, IFN-λ2 and IFN-λ3) IFNs (58,60). They are distinguished by the specificity of their cognate receptors, their primary amino acid sequence homology, genetic locus, stimulus and producing cell type (57). Generally, IFNs are produced in response to both microbial and self-nucleic acids detected in the phagosome, endosome or cytosol of innate immune cells. These cells, once activated, induce a family of IFN specific transcription factors known as interferon response factors (IRFs) (56). The regulation and production of IFNs seem to be linked to which IRFs are being expressed. IRF 1, 3, 5 and 7 appear to be particularly important in the induction of IFN-α gene expression (61), whereas upon receptor activation, IRF3 is important in the induction of IFN-β gene expression, together with NF-κB, which is not involved in IFN-α gene expression (61).

Type I IFNs were initially described as important for anti-viral defense (56). Nevertheless, type I IFNs are believed to be central for pathogenesis (41) and considered to have pleiotropic effects

on cells, as they can induce an antiviral state, inhibit cell proliferation, modulate cell fate (survival/apoptosis), differentiation and migration. Their effects can be local, at the site of production, or systemic (57). All type I IFNs signal through the same receptor, composed of IFNAR1 and IFNAR2 (62), and it is notable that type I IFNs are rarely produced singly. The IFNAR1 chain of the receptor is considered the ''signal transducing chain'' binding a particular IFN-α subtype and IFN-β, whereas the IFNAR2 chain is the high affinity binding chain (63,64).

The amplitude of IFN signalling must be tightly regulated to prevent a harmful immune response. For example, type I IFN production is negatively regulated by surface receptors such as BDCA-2 and ILT7, in human pDCs, which suppress the ability of pDCs to produce type I IFN in response to TLR ligands (65). Additionally, the capacity of pDCs to produce very high levels of type I IFNs may be linked to their constitutive IRF7 expression, which in other cells is usually low and must be primed by an initial burst of IFN-β before optimal levels of other type I IFNs are produced (66).

Besides producing type I IFNs, pDCs can also secrete other pro-inflammatory cytokines such as IL-6, TNF-α, and chemokines, including CXC-chemokine ligand 8 (CXCL8), CXCL10, CC chemokine ligand 3 (CCL3) and CCL4 (8). Here, IL-6 and TNF-α regulate T, B, NK cell and cDCs responses, together with IFN-α and IFN-β (28). By producing IL-6 and type I IFNs, pDCs can also induce the differentiation of B cells into immunoglobulin-secreting plasma cells and instruct plasma cells to preferentially secrete IgG rather than IgM (52). More, type I IFNs and IL-12 promote multiple T cell functions including long-term T-cell survival, memory, $CD8^+$ T-cell cytolytic activity (67), IFN-γ production and increase NK cell-mediated cytotoxicity (68). By producing chemokines, pDCs can attract activated $CD4^+$ and $CD8^+$ T cells to sites of infection (69). Here, pDCs have the potential to impact multiple aspects of innate and adaptive immune responses to viruses (11). Also, accumulating evidence from previous studies suggested that TNF-α play an important role in pathogenesis (70), being produced by Myd88-NF-κB pathway (71). However, this TNF-α expression is upregulated by TLR-4 (70), that is not expressed on pDCs (72). Accordantly, pDCs do not express TNF-α upon activation (73).

As with type I IFN, certain cytokines are important mediators regulating the immune response. IL-1β is one of the most relevant regulating cytokines, since it can mediate a wide range of proinflammatory activities in several human diseases, playing several functions in immune defense. IL-1β is transcribed as an immature pro-peptide, which must be proteolyticaly activated by caspase-1 (74,75). Caspase-1 is triggered after formation of the so called 'inflammasomes'. Inflammasomes are formed upon danger-associated or PAMP recognition (76) and are defined as multiprotein

complexes that recruits the assemble of Nod-like receptors (NLRs). This assemble turn them able to bind the adaptor apoptosis-associated protein, inducing the autocleavage of caspase-1 and production of IL-1-like cytokines. This leads to high concentrations of proinflammatory inflammasome-related cytokine, such as IL-1α/β and IL-18 (74,77).

Type I IFN possess strong inflammatory properties contributing to the inflammasome-dependent caspase-1 activation, leading to proinflammatory pyroptotic cell death. Pyropoptosisis associated with production of IL-1β and IL-18, increases the proinflammatory microenvironment in infected and wounded tissues (78). These cytokines may be secreted by immune cells such as DCs (77). As with other immune responses, uncontrolled IL-1β production may cause damage to host tissues and exacerbate pathologies with an inflammatory component (74), such as psoriasis that increases the caspase-1 activity, suggesting inflammasome activation (79).

TLR recognition of ligands culminates in downstream secretion of chemokines and cytokines, such as IL-1β pro-form (74). Additionally, a synergy seems to exist between type I IFN and TNF pathways, with a reciprocal regulation, since the lack of IFN-α/β signaling did not reduce the induction of TNF-α, IL-1α or IL-1β. Also, MyD88 requirement in the induction of all proinflammatory genes demonstrates an important role for signaling through TLRs (80).

pDCs seem to be linked with IL-1β induction since their depletion affect the production of TNF-α, IL-1α, and IL-1β mRNA (80), whereas their presence promotes IL-1β release, indirectly helping to contain infections (81).

DC Activation

Production of type I IFNs by pDCs occurs after TLR-7/-9 triggering (28) augmenting the expression of antiviral molecules and promoting apoptosis of virally infected cells (82). This IFN secretion by pDCs is recognized by rapid kinetics, high level (up to 1000-fold higher than most cells) and appears critical for innate immune responses against many viruses (1).

TLRs are a set of type I transmembrane proteins evolutionarily conserved among insects and vertebrates, of which at least 10 members have been identified in humans (5). They are membrane-

spanning molecules that contain an ectodomain of leucine-rich repeats, a transmembrane domain and a cytoplasmic domain known as TIR (Toll/IL-1 receptor) domain (28).

Dendritic cells sense viral infections through a subset of nucleic acid–recognizing TLRs, with human pDCs selectively expressing TLR-7 and TLR-9 (34). pDCs TLR-7 and TLR-9 are expressed within endosomal compartments and detect nucleic acids derived from viruses, bacteria, or dead cells. Engagement of TLR-7 and -9 with their ligands (RNA or DNA, respectively) triggers a downstream signaling cascade (28). TLR-9 senses double-stranded (ds) DNA viral genomes rich in unmethylated CpG sequences or phosphodiester backbone in natural DNA, as well as synthetic CpG oligodeoxyribonucleotides (CpG ODN). TLR-7 detects viral single-stranded (ss) RNA and synthetic oligoribonucleotides (ORN), that includes uridine-rich ssRNA, synthetic imidazoquinolines and guanosine analogues (11,17,34).

TLR-9 and TLR-7 are synthesized in the endoplasmic reticulum and transported into endosomes, where TLR-9 is converted into an active form by proteolytic cleavage (83). Compartmentalization of TLR-9 facilitates the interaction with foreign DNA and decreases the risk of contact with self-DNA which can ultimately lead to the development of autoimmune diseases (32). Thus, the endosomal location of TLR-9 prevents immune responses to extracellular self-DNA because this DNA fails to enter the cells spontaneously (5). The delivery of viral nucleic acids into intracellular endosomes containing active TLR-9 and TLR-7 requires a tight spatiotemporal regulation of membrane trafficking (84). Such regulation can be observed for TLR-7 and TLR-9 upon microbial activation, as they travel to the endosomes to become proteolytically activated (17,28,30). Spatiotemporal regulation is critical for a high-level IFN induction in response to TLR-9 activation (84), given that the recognition of nucleic acids by endosomal TLRs requires the maturation and acidification of the endosomes (19). For this, the IFN-inducing TLR-9 ligand is retained for long periods in the endosomal vesicles of pDCs (84). There are several chaperone proteins involved in TLR egress control from ER. For example, the multi-transmembrane endoplasmic reticulum resident protein UNC93B. This protein specifically interacts with the transmembrane domains of TLR-7 and TLR-9 and controls their delivery to the endosomes upon activation (17,28,30). Here, UNC93B delivers TLR-7/-9 from the endoplasmic reticulum to endolysosomes where the ectodomains of TLR-7/-9 are cleaved by cathepsins and asparagine endopeptidase to generate functional TLRs for ligand recognition (85).

MyD88 serves as a key adaptor molecule that functions to recruit IL-1-receptor associated kinases (IRAKs) to almost all TLRs and to the IL-1 receptor (86). MyD88 binding to TLRs then initiates a multiple signaling pathway, such as NF-κB, mitogen-activated protein kinases (MAPKs) and IRFs, and initiates the production of cytokines, chemokines and co-stimulatory molecules (28) (Figure 1). This response is dependent on cell type. In pDCs, MyD88-dependent pathways mostly induce an enormous amount of type I IFNs or proinflammatory responses, such as production of TNF-α, IL-6 and IL-12 (60). Here, in the first 6hours following TLR-7/-9 activation, pDC devote up to 60% of their transcriptome to expression of type I and type III IFN genes. Such capacity requires specific cellular and molecular mechanisms. The rapid IFN-α/β production is mediated by constitutive expression of IRF7 (87). The activation of this pathway causes large pre-made quantities of IRF7 (which is unique for this cell type) to dimerize (88).

There are some synthetic ODNs expressing CpG motifs that are able to trigger an innate immune response via TLR-9 (98). Activation of human pDCs with CpG ODNs is well-established (99,100), being the major effectors of this response (73). CpG ODNs can be divided in two structurally distinct classes that activate pDCs: CpG-A (known as "D" ODNs) that induce the secretion of IFN-α by pDCs that then activate NK cells, which stimulate IFN-γ production; and CpG-B (also referred "K" ODNs), that triggers the production of TNF-α and IL-6, inducing B-cell proliferation and antibody production (98,101). These studies suggest that pDCs may have developed two different signaling mechanisms to respond to different types of CpG ODN. CpG binds to the cell surface, enters the cell by means of clathrin-dependent pathways and is recognized by TLR-9 located in the endoplasmic reticulum and endosomal compartments. TLR-9 responds to different types of ODNs, which is in part dependent on sequence motifs and secondary structures (102). Here, CpG-B are linear single-stranded polynucleotides that express multiple unmethylated CpG motifs, triggering a NF-kB-dependent proinflammatory response characterized by the production of IL-6 and TNF-α by pDCs. In contrast, CpG-A form complex stem loop structures and have a poly-G tail that leads them to form G-tetrads, which stimulate pDCs to produce IFN-α/β rather than TNF-α, an effect that is amplified though an autocrine feedback loop (28). Here, synthetic oligodeoxynucleotides expressing such CpG motifs mimic the ability of bacterial DNA to stimulate pDCs (18).

TLRs are established as the main innate receptors in pDC activation. However, studies began to exploit the impact of cytosolic nucleic acid sensors on type I IFN or pro-inflammatory cytokine production by pDCs. Recently it was shown that several CpG ODNs can also link cytosolic receptors, mediating immune responses. CpG-A oligonucleotides bind selectively to the (DExD/H)-box helicase

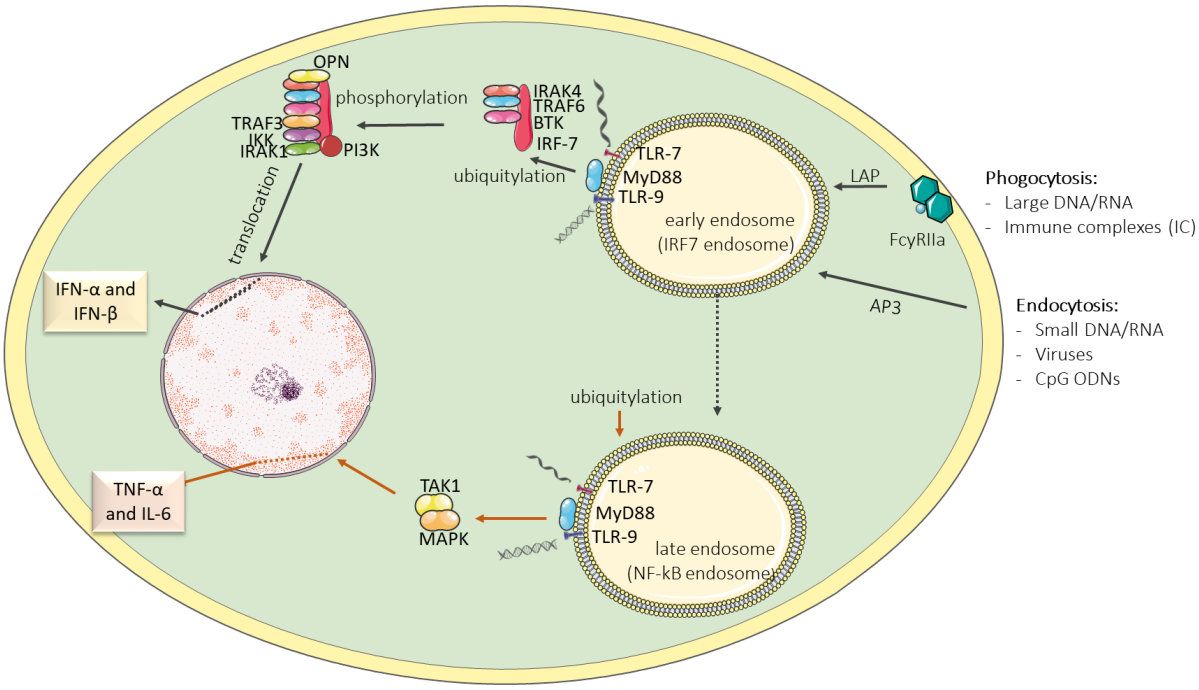

Figure 1 - Cytokine production upon TLR-7/9 induction of MYD88–IRF7 and MYD88–NF-κB pathways. *Trafficking of TLR-9 to the subcellular compartment for type I IFN production is dependent on adaptor protein 3 (AP3) (89). However, TLR-9 mediated recognition of large DNA-containing immune complexes is independent of AP3 and requires the convergence of phagocytic and autophagic pathways. This process is called microtubule-associated protein 1A/1B light chain 3 (LC3)-associated phagocytosis (LAP) and involves autophagy-related proteins but not the conventional autophagic pre-initiation complex (90). In the absence of PAMPs, TLR-9 resides in the endoplasmic reticulum of resting pDCs and is only translocated to the endosomal compartment on exposure to TLR agonists. TLR linkage with the early endosomal/lysosome-related compartment will preferentially lead to IFN production, whereas late endosomal/lysosomal engagement induces pro-inflammatory cytokine production and maturation (89). Thus, production of type I IFN or pro-inflammatory cytokines depends on the type of compartment in which these TLRs encounter their ligands (43). After ligand engagement, activation of TLR-9 by nucleic acids leads to the recruitment of the adaptor protein MyD88 and to the assembly of a multiprotein signal transduction complex in the cytoplasm (91). The signaling cascade downstream forms a multiprotein signal transduction complex that contain IL-1 receptor-associated kinase 4 (IRAK4), TNF receptor-associated factor 6 (TRAF6), Bruton's tyrosine kinase (BTK) and IRF7 (17). Here, IRF7 is activated through ubiquitylation by the ubiquitin E3 ligase activity of TRAF6 and phosphorylated by IRAK4 (92). Phosphorylated IRF7 interacts with TRAF3, IB kinase (IKK), IRAK1, osteopontin (OPN) and potentially phosphatidylinositide 3-kinase (PI3K), and is then translocated into the nucleus where it initiates the transcription of type I IFN genes (80,93,94). Simultaneously, TRAF6 complex may ubiquitylate the protein kinase transforming growth factor-β (TGF-β)-activated kinase 1 (TAK1), (95,96) a signal transducer that activates NF-κB and MAPKs for the induction of transcription of pro-inflammatory cytokines, chemokines and co-stimulatory molecules (28,97). Thus, activation of these TLRs can mediate two different pathways: MYD88–IRF7 pathway and MYD88–NF-κB pathway (8).*

DHX36, associated with translocation of IRF7 to the nucleus and type I IFN production in pDCs, whereas CpG-B oligonucleotides are bound by DHX9, resulting in NF-κB activation and secretion of pro-inflammatory cytokines (103). Similarly, pDCs also express two cytosolic sensors for viral RNA, namely RIG-I and MDA5 (104). Uptake and recognition of viral nucleic acids by pDCs may probably occur independently of viral infection mechanisms. Here, viruses and endogenous nucleic acids can enter pDCs through Fc receptors when bound by antibodies during an immune response, specifically activating the Fc receptor FcγRIIA (40).

Activation by self-DNA immune complexes

pDCs are activated by DNA of viruses and other TLR-9 ligands, such as CpG-A. However, not only viral nucleic acids activate pDCs (19), but self-DNA somehow also access the TLR-9-containing intracellular compartments, triggering a type I IFN response. pDCs normally do not respond to the host-derived self-DNA that typically is released into the extracellular environment by dying cells. However, it was recently shown that self-nucleic acids can form complexes with a cationic antimicrobial peptide LL37 (48). LL37 is produced in skin wounds and overexpressed in psoriasis, a common autoimmune disease of the skin (5). Antimicrobial peptides (AMPs), such as LL37, are found both in nonvertebrates and vertebrates, allowing efficient lysis of the invading microbes (89). LL37 is also considered as a Host-defense peptide (HDP) (105). AMPs are one of the defense mechanisms of eukaryotic cells against bacteria, protozoa, fungi, and viruses, and are produced at damaged epithelial surfaces, preventing microbial invasion by directly killing pathogens through their cationic and amphipathic structure, interacting and disrupting microbial membranes, which typically contain negative charges (106). The main AMPs in human skin are the defensins, which comprise multiple cysteine-rich beta-sheet peptides, and the cathelicidins, a peptide family with only one member with α-helical structure. LL37 is included in cathelicidins, playing a major role in initiation of inflammation in response to skin damage by infection or injury (107). High LL37 concentrations affects cell viability, and thus the function of LL37 requires tight regulation (108). The antibacterial activity is regulated by environmental changes in osmolarity or pH, which relates to the fact that LL37 adopts an α-helical oligomeric conformation in its active state (109). In DCs, LL37 was found to profoundly influence the exact course of their maturation process, a process which forms the borderline between innate and adaptive immunity (110). LL37 owes its name to its 37-amino acid length, initiated by two leading leucine residues, not containing any cysteine residues. This is the only known human cathelin-associated antimicrobial peptide and belongs to the class of α-helical AMPs (110,111). This peptide has been shown to be secreted by multiple cell types (111), being first described in leukocytes and testis, but being later found in a large variety of cells, tissues and body fluids. Thus, LL37 and its precursor hCAP18, can be found at different concentrations in very different cell and tissue types and body fluids (110).

LL37 is present in the dermal compartment in close association with high numbers of pDCs and is produced and secreted by keratinocytes and neutrophils as part of hCAP18 and cleaved into

the mature (biological active) 37-amino-acid AMP by serine proteases. However, LL37 is not expressed by healthy skin keratinocytes, but only following skin injury (48).

Crucially, LL37 mediates pDCs activation by converting self-DNA into structures that are sequestered in endosomal compartments where they trigger type I IFN production through TLR-9 (48), as shown in autoimmune diseases (37). LL37 is able to form complexes with self-DNA, enabling efficient internalization of DNA to mammalian cells, by binding DNA via nonspecific electrostatic interactions (109). Within these complexes, LL37 protects DNA from endonucleases and facilitates the delivery of nucleic acids into the endosomal and cytosolic compartments (109,112). The degree of IFN-α production may be modulated by the efficiency of endosomal access. Also, immunocomplexes can cross-link multiple TLR-9 receptors, leading to receptor recruitment and amplification of the immune response (56).

As a complex, LL37 and DNA together can trigger an over and continuous IFN response in pDCs, leading to the initiation and maintenance of autoimmune skin inflammation (5). This phenomenon involves three distinct steps. First, LL-37 binds to DNA fragments to form aggregated and condensed structures that are resistant to extracellular degradation. Second, LL-37 promotes DNA translocation into the endocytic compartment of pDCs, thereby bypassing a safety mechanism for discrimination of viral/microbial from self-nucleic-acids provided by the intracellular localization of TLR-9. This process involves the attachment of LL-37 to proteoglycans in the cell membrane followed by lipid-raft mediated endocytosis, an entry mechanism described for certain viruses. Finally, LL-37 retains the DNA complex in early endocytic compartments of pDCs, perhaps modifying them in the process, to specifically sustain the TLR-9-mediated IFN response. Thereby, LL-37 breaks innate tolerance to self-DNA and, in a similar way to viral responses, elicits a rapid and robust induction of IFNs that initiate innate and adaptive immunity, allowing a selective and sustained IFN induction via TLR-9/MyD88/IRF7 signaling (5,48).

The immunogenicity of LL-37 is entirely dependent on its positive charges clustered on one side of the molecule that neutralizes the negatively charged phosphate backbone of DNA, leading to DNA condensation to small particles that are protected from nuclease degradation. These DNA particles acquire a slight positive charge as some cationic residues of the complexed peptide remain exposed, allowing interaction of the complex with heparin sulfate proteoglycans in cell membranes, followed by internalization via endocytosis (113). New evidences suggest that the inter-DNA spacing is an important criterion for pDC activation in these complexes, since LL-37–DNA complexes seem to

have a columnar structure with a relatively large inter-DNA spacing (a=3.40 nm) (56). Recent evidence suggests that HMGB1, a DNA-binding factor released by dying cells, can bind only multimeric aggregates. HMGB1 may bind LL-37-self-DNA complex, promoting prolonged association with TLR-9 in early endosomes by engaging the receptor of advanced glycation endproducts (RAGE). The complex is protected from nuclease degradation and delivered to endocytic compartments of pDCs to TLR-9 retention within early endosome, leading to a robust induction of type I IFNs that initiate an antiviral-like immune response (56). More, in pDCs LL-37-DNA complexes are contained within the early endosomes (112) and their uptake is a saturable time- and temperature-dependent process (no DNA uptake at 4 °C), which is consistent with an endocytotic uptake mechanism (109).

In context of SLE, HMGB1 is released from cells undergoing necrosis or is secreted from cells after inflammatory cytokine stimulation (114). In addition, in SLE, self-DNA–LL37 complexes are released by dying neutrophils undergoing NETosis, a cell death process in which activated neutrophils extrude nuclear DNA into the extracellular space in the form of NETs. NETs may serve as a source of autoantigen and LL37, promoting aggregation and stimulation of IFN-α by pDCs (115). This raises the possibility that HMGB1 may contribute to autoimmune disorders characterized by type I IFNs, through a mechanism dependent on MyD88–TLR-9 pathway and RAGE. Moreover, HMGB1 seem to be present in immune complexes with DNA and to trigger type I interferon production after RAGE engagement (41).

IL-1β also seem to be related with autoimmune diseases, such as psoriasis (79), where a role for LL37 seem to exist. In fact, LL37 peptide may enhance IL-1β induction by some cell types (5,19). LL37 can regulate the release of IL-1β secretion stimulus in monocytes, linking the innate and the adaptive immune system (75) and seems to induce inflammasome formation, in a process independent of TLRs and IRFs (116). The self-DNA present in keratinocytes in psoriatic lesions was also found to have pro-inflammatory response induction and to triggers IL-1β secretion through the AIM2 inflammasome. However, binding of LL37 to self-DNA neutralizes this DNA-mediated inflammation. Therefore, LL37 shows opposite roles in skin inflammation in psoriasis (76). Thus, LL37 can also block inflammasome formation by binding to cytosolic DNA (105). However, not much is known of how the activity of cytosolic LL37 is regulated and neither about the role of CAL-1 cells in inflammasome, leading space for further investigation.

Self-RNA–LL37 complexes also trigger the direct activation of mDCs to secrete TNF-α and IL-6 and differentiate into mature DCs. Again, the formation of the complexes is driven by the cationic

residues of LL37 and the anionic phosphate backbone of RNA, similar to the phenomenon described for DNA. Thus, LL37 allows the association of RNA with cellular membranes and the transport across these membranes into endocytic compartments (34). Other molecules have similar effects, being able to condense self-DNA into particles capable of being endocytosed by pDCs, leading to activation of TLR9. Some of them are hBD2, hBD3, and lysozyme, and, like LL37, are found in skin injury and found to have inducing IFN production skills (113).

Mitochondria have circular DNA genome containing unmethylated CpG oligodeoxynucleotide (ODN) sequences. Mitochondrial DNA (mtDNA) molecules released by injured or even living cells are sensed as danger signals, initiating immune responses (117). Recently, it was shown that mtDNA and LL37 are also involved in atherosclerosis, as high amounts of LL37-mtDNA complex were found in atherosclerotic plasma and plaques. LL37-mtDNA complex was also found to cause inflammation by activation of TLR-9-mediated inflammatory responses (53). LL-37 has been identified residing in neutrophil and NETs in atherosclerotic lesions and, both nDNA and mtDNA are present in NETs and dying cells, allowing the formation of either LL-37-nDNA and/or LL-37-mtDNA complexes. The formation of either the nDNA or mtDNA complexes are thought to play a similar role (53). mtDNA contains similar unmethylated CpG repeats to bacterial DNA, leading to augmented secretion of IFN-α with LL37-mtDNA in comparison to LL37-nDNA. Thus, the LL37-mtDNA complex might display stronger inflammatogenic properties than LL37-nDNA and might be highly inflammatory in vivo (53,54). LL37-mtDNA complex was retained in the loading wells, suggesting that LL37-mtDNA complex is resistant to DNase II digestion. mtDNA alone could be easily degraded, which imply that LL37 protects mtDNA from degradation. More, LL37-mtDNA stimulation increased the number of TLR-9-positive endosome, triggering activation of TLR-9 and secretion of chemokines and cytokines. This leads to an exacerbate inflammation by stimulating IFN-α production in pDCs (53).

mtDNA is susceptible to oxidation, a proinflammatory modification detected in SLE sera. LL37 complexed with oxidized mtDNA (Ox-mtDNA) enables their uptake, resulting in a 10-fold enhance of “normal” TLR-9-dependent IFN-α levels (54). However, another study mentioned that both mtDNA and Ox-mtDNA in complex with LL37, were able to promote IFN-α production by pDCs, but mtDNA complexed with LL37 resulted in significantly more IFN-α release than the oxidized form (117). In pDCs it was also shown that stimulation with mtDNA resulted in a significant increase in expression of CD86, CD83, TFN-α and IL-8, and that phenotypic maturation of pDCs is induced by mtDNA as well as oxidized mtDNA, mediated through TLR-9. Thus, human pDCs may serve as a primary sensor for mtDNA, inducing maturation, migration, and type I IFN production of pDCs (117).

CAL-1 cell line

In 2005, *Maeda et al.* were successful in establishing of a novel cell line, CAL-1, which shares many similarities with pDCs. Primary malignant cells were obtained from the peripheral blood of a patient, a 76-year-old male, who had a skin tumor on his back, whose lymph node biopsy revealed a blastic NK cell lymphoma diagnosis according to the WHO classification, that was later found to have $CD4^+$ $CD56^+$ hematolymphoid neoplastic features (118). $CD4^+CD56^+$ hematodermic neoplasm and blastic NK-cell lymphoma is now called Blastic pDC neoplasm, and is a hematopoietic malignancy of pDC origin (30). The derived cell line, CAL-1 cells, were found to express mRNA for TLR-2, -4, -7 and -9. Also, this cell line does not express lineage-associated markers of CD3, CD14, CD19, CD16, and CD11c but shows positive results for CD4, CD56, CD45RA, HLA-DR, CD123 and CD38. Morphologically CAL-1 are large blastoid cells with agranular prominent basophilic abundant cytoplasm, pale Golgi area, and an eccentric nucleus with 1 or 2 nucleoli. Thus, CAL-1 cells resemble plasma cells, have slight nuclear irregularity with a large nucleolus, abundant mitochondria, and parallel arrays of rough endoplasmic reticulum (RER) but no Russell bodies. These results are similar when the authors compared primary cells and CAL-1 cells in culture. Moreover, both cells are weakly positive for CD11c, CD7 and granulocyte-macrophage colony-stimulating factor-α (GM-CSFα), positive for CCR5 and for CXCR4 and CXCR3. CAL-1 cells can change morphologically into the mature DC phenotype after short-term culture in the presence of GM-CSF and IL-3. Three days after exposure to GM-CSF or IL-3, cells exhibit many long dendrites, leading to a weak up-regulation of expression of CD11c, CD13, and CD33 and down-regulation of CXCR3 and CXCR4. CD80 and CD86, which are either not expressed or present on unstimulated CAL-1 cells, are up-regulated upon 3 days of culture in the presence of IL-3. After stimulation with the TLR-9 ligands CpG ODNs, the cells produce significant levels of TNF-α and a small amount of IFN-α, showing some aberrant features, maybe due to their tumorigenic origin (118). Thus, CAL-1 cells are closely related to the pDC lineage while having some phenotypic characteristics different from those of pDCs, namely: a more blastoid morphology with large nucleoli; expression of CD33, CD7, and CD86, mRNA expression of TLR-2 and TLR-4; and responsiveness to IL-3 and GM-CSF (118).

Upon activation, CAL-1 cells can also produce large amounts of type I IFNs and some other proinflammatory cytokines through TLRs/MyD88 signal pathways. More, CAL-1 cells present several IRFs including IRF-1, IRF-3, IRF-5, IRF-8 and NF-Kb p50, which are key regulators of IFN-β and IL-6 expression following TLR-9-mediated activation (35). Besides the activation of TLR-9 pathway, the

stimulation of CAL-1 with mimetics for exogenous RNA leads to activation of TLR-7, also resulting in induction of proinflammatory cytokines (IL-6 and TNF-α) as well as type I IFN (119). Human CAL-1 pDC-like cell line can thus provide novel insights into regulation of TLR-7 and 9-mediated activation of human pDCs. CAL-1 cells mimic the response of human pDCs to CpG-B stimulation, triggering translocation of IRF-5 from the cytoplasm to the nucleus, increasing expression of mRNA encoding several IRFs. IRF-5 (but not IRF-1) contributes to CpG-B upregulation of IFN-β and IL-6 in human pDC, and IRF-8 negatively regulates expression of these genes. These regulation factors both complex with MyD88 in resting CAL-1 cells (120).

In conclusion, CAL-1 cells share many phenotypical similarities with pDCs as well as other functional characteristics such as nucleic acid recognition, TLR-9 triggering upon stimulation and cytokine expression, which is interesting in establishing CAL-1 cell line as a pDC model. Due to the paucity of circulating primary pDC, having a cell model is crucial to study the molecular mechanisms that may trigger and ensue progression of the autoimmune diseases. However, activation of CAL-1 cells with these complexes are not yet studied.

Objectives

The main goal of this thesis is to establish a cell model to study activation of human pDCs with immune complexes. Thus, our specific objectives are to optimize stimulation of the cell line CAL-1 with LL37-self DNA complexes. For activation, we will optimize the concentration of both LL37 peptide and DNA, as well as evaluate activation and the subsequently early endosome and TLR-9 recruitment. We will also analyze possible differences between activation with nuclear DNA or mitochondrial DNA.

II. Materials & Methods

Cell culture

CAL-1 cells were grown in RPMI 1640 medium (Gibco, USA) supplemented with 10% of heat-inactivated Fetal Bovine Serum, 1mM Hepes (Gibco, USA), 2mM L-Glutamine (Gibco, USA), 1mM Sodium Pyruvate (Gibco, USA) and Non-essencial Aminoacids 1x (Gibco, USA) (73). Cells were cultured at 37°C in CO^2 in an air incubator and plated every two days to a cell density of $0.3x10^6$cells/ml. Different sera batch from different suppliers were tested, namely Sigma (F7524, Sigma-Aldrich, USA), PAN Biotech (P30-1401, PAN Biotech, Germany), BioWest (S1810, BioWest, USA), HyClone (SV30160, HyClone, USA), Gibco (10500064, Gibco, USA) and another different one from Sigma, gently provided by Philippe Pierre (CIML, Marseille). Every serum was thawed at 4°C overnight and then inactivated by heat at 56°C for 30minutes. To evaluate CAL-1 growth, the number of cells with each serum was counted at 0h, 24h, 48h, 72h and 96h, starting with the same cell number ($9x10^4$cells). Cell viability was also measured in each time point upon staining with Propidium Iodide (1mg/ml) (Sigma-Aldrich, USA), measured by Flow Cytometry in BD Accuri C6 Cytometer, and compared with the control condition (with no Propidium Iodide). The control condition was used to perform the gating.

Preparation of DNA-complexes

To test activation of CAL-1 cells with immunocomplexes formed with LL37, CAL-1 nDNA and mtDNA were firstly isolated. For nDNA isolation, cells were expanded to obtain a final number of 10^7cells. The pellet of cells was collected by centrifugation at 300g for 6 minutes, and self-nDNA from the pellet was isolated using the NZY tissue nDNA isolation kit (NZYTech, Portugal). First, cells were resuspended in 200µl Buffer NT1. Then, 25µl Proteinase K solution and 200µl of Buffer NL were added and mixed thoroughly by vortexing, and incubated at 56°C for 15minutes (the vortex was used occasionally during the incubation). Next, 210µl of 100% ethanol was added to the sample and mixed immediately by vortex. The mixture was transfer into a NZYSpin Tissue Column placed in a 2ml collection tube and centrifuge for 1minute at 11000g. The supernatant was discarded and the column was placed in a new collection tube. Then, 500µl of Buffer NW1 was added to the column and centrifuged again for 1minute at 11000g. The supernatant was discarded and the column was

placed back into the collection tube. Next, 600µl of Buffer NW2 (with previous addition of ethanol - 28ml of 100% molecular biology grade ethanol to each bottle of buffer NW2) was added to the column and centrifuged again for 1minute at 11000g, then discarding the flow-through and placing the column back into the collection tube. Another centrifugation of 2minutes at 11000g was performed to dry the membrane. Finally, the column was placed into a clean microcentrifuge tube and 100µl of sterile water was added directly in the membrane column, incubated for 1minute at room temperature and centrifuge at 11000g for 2minutes to elute the DNA. DNA quantity and quality were then evaluated with Nanodrop (Denovix, USA). DNA was stored at -20°C.

To isolate mtDNA, cells were expanded to obtain a final number of 10^8cells and then submitted to differential centrifugation. A pellet of 10^8cells was first collected by centrifugation at 300g for 6minutes. The supernatant was discarded and the pellet was washed 2x with PBS and centrifuged at 300g for 6minutes to obtain a clean cell pellet. Then, the pellet was resuspended in 2ml of isolation buffer (10mM HEPES pH=7,5, 250mM Sucrose, 1mM EGTA, 5g/L BSA) and centrifuged at 500g for a maximum of 2minutes. The supernatant was discarded and the pellet was resuspended in 3ml of isolation buffer and homogenized with a potter. Then, the homogenate was centrifuged at 1500g for a maximum of 10minutes. The supernatant was kept and the pellet was homogenized and centrifuged again at 1500g for a maximum of 10minutes. The supernatant was added to the supernatant obtained previously and centrifuged at 10000g for a maximum of 10minutes. The resultant mitochondrial pellet was washed with isolation buffer without BSA (121). After isolation of the mitochondrial fraction, mtDNA was isolated using the NZY tissue nDNA isolation kit (NZYtech, Portugal), as described earlier, and kept at -20°C.

Some authors refer that complexes can be generated by mixing 1µg of self-nDNA with 10µg LL37 (final concentration of 50µg/ml or 10µM) (34). Here, a titration was performed to determine the best concentration of LL37 and DNA to activate CAL-1 cells.

Immunocomplexes of nDNA with LL37 peptide (InvivoGen, USA) (LLGDFFRKSKEKIGKEFKRIVQRIKDFLRNLVPRTES-C') were thus prepared to test the best concentration of LL37. Here, 1µg/ml of nDNA was used to prepare complexes with four different final concentrations of LL37 (50µg/ml, 20µg/ml, 10µg/ml and 5µg/ml). Immunocomplexes were prepared first in 20µl of PBS for 30 minutes at room temperature and then diluted into 200µl of complete medium (34).

To test the best quantity of nDNA and mtDNA to use in the immunocomplexes, different concentrations of both nDNA and mtDNA were used, namely 1µg/ml, 0.5µg/ml and 0.2µg/ml of

nDNA/mtDNA, both with 10µg/ml of LL37, except in the first that stimulation was tested, where was only tested one concentration of 0.5µg/ml of mtDNA.

Cell stimulation

CAL-1 cells have some particularities regarding its stimulation, being necessary to reduce the serum concentration before stimulation. Here, new RPMI 1640 medium was prepared but this time supplemented with 1% of heat-inactivated FBS (119). To test activation, cells were washed by centrifugation at 1200rpm (~300g) for 6minutes and counted in a neubauer chamber with Trypan Blue (Sigma-Aldrich, USA). Then, cells were resuspended in medium with 1% FBS in a cell density of $1x10^6$cells/ml (122). Cells were incubated overnight (12-16h) at 37°C in CO_2 in an air incubator, containing 1ml of cell suspension for each condition, in a 24-well plate. Cells were mycoplasma free.

To select a serum batch, after the overnight incubation, cells were stimulated with 3µM CpG-ODN 2216 (Tebu-bio, France) (122) at different time-points (3h, 6h and 9h) (73) comparing to a control condition with no stimulation (0h) and cultured at 37°C in CO_2 in an air incubator. After each time-point, the cell pellet was collected by centrifugation at 1200rpm (~300g) for 6minutes, to further mRNA evaluation.

To test the activation of CAL-1 cells with immunocomplexes of DNA with LL37, cells were seeded in a well of 24-well plate and cultured overnight (12-16h) with 1% FBS medium (*Sigma-Aldrich, USA*), before setting up the experiment. As before, cells were seeded at 10^6cells/ml. Thus, $0.75x10^6$cells were cultured in 550µl of 1% FBS supplemented RPMI 1640 medium in a well of 24-well plate and cultured overnight (12-16h) at 37°C in a CO_2 in air incubator. Then, 200µl of medium containing the immunocomplexes were added to the cells in culture. Two different time-points were tested: 6h to evaluate the expression of cytokines mRNA (IFN-α, IFN-β and TNF-α) by RT-qPCR and 24h to evaluate the cytokines secretion by ELISA. Some conditions were also tested as a control, namely cells alone, cells only with the addition of nDNA, cells only with the addition of LL37, all in parallel with 3µM CpG-A ODN 2216 (73) activation to compare the activation pattern. When it comes to mtDNA experiment, mtDNA alone was also added as a control.

After each time point for immunocomplexes, the content of every well was collected and placed in a different microcentrifuge tube and an aliquot of 50µl was saved to perform a viability

test. Cell viability was measured for each time point by Propidium Iodide (Sigma-Aldrich, USA) staining, measured by Flow Cytometry in BD Accuri C6 Cytometer. The remaining volume was centrifuged for 6minutes at 300g. The supernatant was stored and separated in four different aliquots of 120µl to evaluate the cytokines production by ELISA. The pellet was also stored to isolate the RNA and evaluate the cytokine production by RT-qPCR.

Measuring RNA levels by qPCR

RNA from each sample was isolated using the RNeasy Mini Kit (Qiagen, Germany). Here, to the cell pellet collected by previous centrifugation, 350µl of Buffer RLT and the same volume of 70% ethanol and was added, mixing well by pipetting. Then, up to 700µl of the sample was transferred, including any precipitate, to an RNeasy Mini spin column placed in a 2ml collection tube, and centrifuged for 15seconds at 10000g. The flow-through was discarded and DNase digestion was proceeded. Here, 350µl Buffer RW1 was added to RNeasy column and centrifuged for 15seconds at 10000g. The flow-through was discard. Then, DNA digestion was proceeded using the RNase-Free DNase Set (Qiagen, Germany). Here, a DNase I incubation mix containing 10µl of DNase I stock solution and 70µl Buffer RDD was first prepared for each sample and mixed gently by inversion of the tube and centrifuged briefly. After the centrifugation, 80µl of the mix was directly put on RNeasy column membrane and left placed on benchtop (20–30°C) for 15minutes. To conclude the DNA digestion steps, 350µl of Buffer RW1 was added to RNeasy column, centrifuged for 15seconds at 10000g and the flow-through was discarded.

Then, 500µl of Buffer RPE was added to the RNeasy spin column and centrifuged for 15seconds at 10000g, discarding the flow-through. After that, 500µl of Buffer RPE was added to the RNeasy spin column and centrifuge for 2minutes at 10000g. The column was placed into a new 2ml collection tube and centrifuge at full speed for 1minute to dry the membrane. The column was transferred again, this time into a new 1.5ml collection tube, 40µl RNase-free water was directly put in the column membrane and centrifuged for 1minute at 10000 g to elute the RNA.

All the RNA samples were obtained with RNeasy Mini Kit (Qiagen, Germany), except for the samples where the quantity of LL37 in the immunocomplexes was tested. Here, another kit was used, namely NZY Total RNA Isolation kit (NZYtech, Portugal). Before starting the procedure, for each

sample, 10µl of 2-mercaptoethanol need to be added to 1ml of Buffer RLT before use and four volumes of ethanol (96-100%) need to be added to Buffer RPE for a working solution. After collect the pellet samples, 350µl of buffer NR and 3.5µl β-mercaptoethanol were added to the pellet and vortexed vigorously. Then, the lysate was put into an NZYSpin homogenization column placed in a 2ml collection tube and centrifuged for 1minute at 11000g, saving the flow-through. The flow-through was placed into a new 1.5ml microcentifuge tube and 350µl of 70% ethanol was added and mixed immediately by pipetting up and down (not centrifuging). The lysate was loaded in n new NZYSpin Binding column and centrifuged at 11000g for 30seconds. The flow-through was discarded and the column placed into a new collection tube. Then, 350µl of Buffer NI was added and centrifuged at 11000g for 30seconds, the flow-through was discarded and the column was placed back into the collection tube.

To purify the RNA content, DNA digestion was proceeded. For each sample, a Digestion Mix was prepared using 10µl of DNase I and 90µl of digestion buffer. In the center of the silica membrane of the column, 95µl of the Digestion Mix was directly added and incubated at room temperature for 15minutes. After the incubation, 200µl of Buffer NWR1 was added and centrifuged for 1minute at 11000g. The supernatant was discard and the column was placed in a new collection tube. Then, 600µl of Buffer NWR2 was added and centrifuged at 11000g for 1minute, discarding the flow-through and placed the column back in the collection tube. This step was repeated, washing the membrane with 250µl of Buffer NWR2 again and centrifuged at 11000g twice for 1minute to dry the column membrane. The flow-through was discarded, the column was placed in a clean 1,5ml RNase-free microcentrifuge tube and 50µl of RNase-free water was added directly to the column membrane. Finally, the sample was centrifuged at 11000g for 1minute to elute the RNA.

After isolation, the quantity and the quality of the RNA was measured with the nanodrop, using nuclease-free H_2O as control. The resultant A260/280 ratios were between 1.9 and 2.1. The resultant RNA was saved at -80°C.

To evaluate cytokines mRNA expression, cDNA synthesis for each condition needed to be prepared in order to perform the RT-qPCR.

To perform the reverse transcription (cDNA synthesis), one microcentrifuge tube for each condition was prepared, containing 500ng of RNA of each sample, 1µl of dNTP Mix 10mM (NZYtech, Portugal), 2µl of random hexamers (100ng/µl) (Invitrogen, USA) and nuclease free water (Fisher Scientific, USA), for a final volume of 20µl. The content of the tubes was mixed well and then the mixture was heated to 65°C for 5minutes, followed by a quick chill on ice of approximately 2minutes.

The samples were centrifuged briefly and 7µl of the above mix was added to each sample and mixed gently, followed by an incubation of 2minutes at 25°C. Finally, 1µl of SuperScript II RT (Invitrogen, USA) was added, mixed gently and the final mix was put in a thermocycler to perform the reverse transcriptase cycle (incubate for 10minutes at 25°C, followed by 50minutes at 42°C; reaction inactivation by heating at 70°C for 15minutes, followed by 4°C incubation). The resultant cDNA in the tubes were kept at -20°C.

RT-qPCR was performed with the primers (all from Invitrogen, USA) on Table 1.

Table 1 – *Primer sequences for each target gene.*

Gene	*Sequence*
GAPDH – Forward	5'-CAATGACCCCTTCATTGACC-3'
GAPDH - Reverse	5'-TCTGGTCATGAGTCCTTCCA-3'
IFN-α – Forward	5'-TGATCCAGCAGATCTTCAAT-3'
IFN-α – Reverse	5'-CAGCTGCTGGTAGAGTTCA-3'
IFN-β – Forward	5'-TGCTTGGATTCCTACAAAGA-3'
IFN-β – Reverse	5'GGATGTCAAAGTTCATCCTG-3'
TNF-α – Forward	5'-CCCTCAGCAAGGACAGCAGA-3'
TNF-α – Reverse	5'-AGCCGAGGGTCAGTATGTGAG-3'

For qPCR, to each well it was added a mix containing 2µl of cDNA (diluted 1:10), 10µl of SYBR Premix (Clontech, USA), 0.4µl of PCR forward primer, 0.4 µl of PCR reverse primer, 0.08 µl of ROX Dye (Clontech, USA) and 7.12µl of nuclease-free H_2O, in a final volume of 20µl per well.

The plate was centrifuged for 2minutes at 1000g. The qPCR was proceeded using the standard run (initial denaturation: 1x 95℃ 30seconds; PCR: 40x 95℃ 5seconds + 60℃ 30-34seconds; and dissociation stage: 30seconds) in a 7500 Real Time PCR System, from Applied Biosystems.

All samples were analyzed using these reagents, except for the third experiment regarding optimization of LL37 concentrations. In this experiment, for reverse transcription, cDNA Synthesis SuperMix (Bimake, USA) was used. For that, 500ng of each sample of RNA (up to 8 µl), 2µl of 5×qRT SuperMix (Bimake, USA) and RNase-free Water up to 10µl were used to produce cDNA. After sample preparation, they were incubated in the thermocycler at 25°C for 10 minutes, then at 42°C for 30minutes for extension, and finally at 85°C for 5minutes to terminate the reaction. The tubes were stored at -20°C or proceeded directly with the RT-qPCR.

For RT-qPCR, the analysis was proceeded in triplicates. To each well, a total of 20µl of a mix composed for 2µl cDNA, 10µl SYBR LowRox (Bimake, USA), 0.6µl PCR forward primer, 0.6µl PCR

reverse primer and 6.8µl H_2O, were added. Once the plate preparation was completed, it was centrifuged for 3minutes at 1000g. Finally, the qPCR was proceeded using the standard run (holding stage: 95℃ 5minutes; cycling stage 40x: 95℃ 15seconds + 60℃ 60seconds; melt curve: 95°C 15seconds + 60°C 60seconds + 95°C 15seconds), in a 7500 Real Time PCR System, from Applied Biosystems.

Measuring cytokine secretion by ELISA

To evaluate secretion of TNF-α or IL-1β, ELISA assays were performed using Human TNF- α or Human IL-1β Mini TMB ELISA Development Kits, respectively (Peprotech, UK). First, 100µl of monoclonal mouse anti-hTNF-α or anti-hIL-1β capture antibody (1x in PBS) was added immediately to each ELISA plate well and incubated overnight at room temperature. Wells were washed four times using 300µl of wash buffer (0.05% Tween-20 in PBS) per well. In the last wash, the plate was inverted to remove the residual buffer and blot on paper towel. Then, 300µl of block buffer (1% BSA in PBS) was added to each well and incubated for at least 1hour at room temperature. After the incubation, the wells were aspirated to remove liquid and washed four times using 300µl of wash buffer (0.05% Tween-20 in PBS) per well.

To make a standard curve for the evaluation of TNF-α, the Human TNF-α Standard solution was diluted, in the plate, from 2000pg/ml to zero in diluent (0.05% Tween-20, 0.1% BSA in PBS). To make a standard curve for the evaluation of IL-1β, the Human IL-1β Standard solution was diluted, in the plate, from 750pg/ml to zero in diluent. Also, 100µl of samples were added to each respective well. The plate was incubated at room temperature for at least 2 hours. The wells were washed four times using 300µl of wash buffer (0.05% Tween-20 in PBS) per well. Then, 100µl of biotinylated rabbit anti-hTNF-α or goat anti-human IL-1β (0.15µg/ml or 0.25µg/ml, respectively) were added and incubated at room temperature for 2hours. The wells were washed again four times and 100µl of Streptavidin-HRP (0.05µg/ml for TNF-α and 0.075 µg/ml for IL-1β) was added. The plate was Incubated for 30minutes at room temperature and 100µl of TMB Liquid Substrate was added to each well after incubation and after the four washes. The substrate was incubated at room temperature for color development for 20minutes. Finally, 100µl of Stop Solution (1M HCl) was added to each

well and the color development was detected with a spectrophotometer (*TECAN Infinite M200*) using 450nm as primary wave with wavelength correction set at 620nm.

To evaluate the secretion of IFN-α, an ELISA assay was performed using IFN alpha Human Matched Antibody Pair (*ThermoFisher Scientific,* USA). First, 100µl monoclonal coating antibody to Human IFN-α (1µg/ml) of the diluted coating antibody was added to each well of the ELISA plate and incubated overnight at 4°C. Wells were washed once using 400µl of wash buffer (0.05% Tween-20 in PBS 1x) per well, and 250µl of assay buffer (5g BSA and 0.5ml Tween-20 in 1L PBS 1x) was added to each well and incubated for at least 2hours at room temperature. After the incubation, the wells were washed twice using 400µl of wash buffer (0.05% Tween-20 in PBS).

To make a standard curve for the evaluation of IFN-α, the Human IFN-α Standard protein (1ng/ml) was diluted, in the plate, from 500 to 7.8pg/ml in Assay Buffer. Then, 80µl of Assay Buffer and 20µl of each sample were added to the sample wells. Also, 50µl of HRP-Conjugate anti-human IFN-α monoclonal antibody diluted in Assay Buffer (1:1000) were added to all wells. The plate was incubated at room temperature for 2hours, on a microplate shaker set at 400rpm. Then, the microwells were washed three times and 100µl of Substrate Solution (1:2 H2O2 in Tetramethylbenzidine) was added and incubated at room temperature for about 10minutes, to allow color development.

The substrate reaction was stopped by quickly pipetting 100µl of Stop Solution (1M Phosphoric Acid) into each well. Finally, the resultant absorbance of each microwell was red on a spectrophotometer (*TECAN Infinite M200*) using 450nm as primary wave with wavelength correction set at 620nm.

Analysis of complex recognition by Immunofluorescence

The evaluation of the immunocomplex entrance within endosomes (rabbit monoclonal antibody anti-EEA1 clone F.43.1, ThermoFisher Scientific, USA) and TLR-9 recruitment (mouse monoclonal antibody anti-TLR-9 clone 26C593, Santacruz Biotech, USA) was performed by immunofluorescence. Here, to identify the complexes, the antibody mouse monoclonal antibody anti-LL37 conjugated Alexa Fluor 488 clone D-5 (Santacruz Biotech, USA) was used. To perform the immunofluorescence experiment, coverslips were first treated with Alcian Blue solution (Sigma-

Aldrich, USA) and heated at microwave until boiling, followed by washing steps first with distillated water, then with ethanol 70% and again distillated water. Then, the coverslips were left drying individually in a paper towel.

After stimulation with the immune complexes, cells were collected and centrifuged for 6minutes at 300g. Then, the cell pellet was resuspended in 1ml of RPMI 1640 (without supplements and FBS) and 50µl were placed on a coverslip pre-treated with Alcian Blue. Cells were incubated for 20minutes in an air incubator at 37°C 5% CO_2. The cells were fixed with 500µl of Paraformaldehyde (PFA) 4% for 10minutes at room temperature, being washed before with PBS 1x and kept in PBS until staining. To permeabilize the cells, the coverslip was covered with 500µl of Permeabilization Buffer (1% glycine (1M), 5% FBS and 0.1% Triton-X) and incubated for 5minutes. After that, buffer was removed and the cells were covered with 500µl of Staining Buffer (1% glycine (1M) + 5% FBS) and incubated for 10minutes.

Different concentrations for the antibodies were tested (Table 2).

Table 2 *- Concentration range for antibody concentration test.*

Antibody	*Concentration*			
Mouse anti-TRL9	1:50	1:100	1:200	1:500
Mouse anti-LL37-AF488	1:100	1:250	1:500	1:1000

To incubate the primary antibodies, a mix was prepared by diluting the antibodies with staining buffer, in a final volume of 50µl/sample, which was added to each coverslip. The coverslips were left incubating for 45minutes at room temperature in a wet chamber. After incubation, the coverslips were washed three times for 5minutes with staining buffer. In the last wash, the staining buffer was not removed.

The monoclonal antibody mouse anti-TLR-9 was detected with the secondary antibody Goat anti-mouse IgG Alexa Fluor 568 (ThermoFisher Scientific, USA) and the monoclonal antibody rabbit anti-EEA1 was detected with Goat anti-mouse IgG Alexa Fluor 647 (ThermoFisher Scientific, USA). To incubate the secondary antibody, a mix was prepared by diluting the antibodies with staining buffer, in a final concentration of 1:500 in 50µl/sample, which was added to each coverslip. The coverslips were incubated for 1hour at room temperature. After incubation, the coverslips were

washed three times for 5minutes with staining buffer. In the last wash, the staining buffer was not removed.

The mouse antibody anti-LL37 conjugated with Alexa Fluor 488 was the last to be added. Again, a mix was prepared by diluting the antibody with staining buffer, in a final volume of 50µl/sample, and was added to each coverslip. The coverslips were left incubate for 1hour at room temperature. Coverslips were washed once with staining buffer and twice with PBS. In the last wash, PBS was not removed and the coverslips was briefly rinsed in distilled water and gently dried in a paper towel before placing on slides with 6µl of ProLong (ThermoFisher Scientific, USA).

After defining the best concentration for each antibody, staining was performed following the indicated concentrations on Table 3. To better understand the stimulation pattern, different time points (0h, 15min, 30min, 60min and 120min) of cell incubation with immunocomplexes were tested to follow progress of stimulation.

Table 3- *Antibody concentration for evaluation of TLR-9 and EEA1 recruitment of immunocomplexes with endosomal internalization.*

Antibody	*Concentration*	*Conjugate*	*Concentration*
Mouse anti-TRL9	1:200	*Goat anti-mouse Alexa Fluor 568*	1:500
Rabbit anti-EEA1	1:200	*Goat anti-rabbit Alexa Fluor 647*	1:500
Mouse anti-LL37-AF488	1:200	-	-

Statistical Analysis

All data regarding RT-qPCR and ELISA assays were statistically evaluated through the *GraphPad Prim®* software v.7.00 (La Jolla, CA, USA*)*. Each experiment was repeated five times. For each condition, a normality test was performed to evaluate if the results came from a Gaussian distribution, using the D'Agostino and Pearson test. Because of the small "n" for each condition, it was not possible to ensure a Gaussian distribution. However, statistical analysis was performed by One-way ANOVA test, assuming normality. No statistically differences were found in all assays.

III. Results & Discussion

Serum batch choice

The behavior of pDCs is dependent on the batch of serum used for cell culture, being crucial to select a serum that allows good cell viability and promotes good conditions to evaluate activation of the cells. In order to find one batch that promoted the best growth conditions, CAL-1 cells were cultured with RPMI 1640 medium supplemented with serum from different suppliers. A serum batch from Sigma that has been previously used by our collaborators (from Marseille) was used as positive control and the number of cells was counted at different time points (0h, 24h, 48h, 72h and 96h), to evaluate the growth of cells in each condition (Table 4 and Figure 2).

Table 4- *Number of cells after culture in medium with 10% sera from different suppliers, at different time-points (0h, 24h, 48h, 72h and 96h). Data was obtained by diluting a cell suspension with Trypan Blue and counting on a neubauer chamber.*

		0h	*24h*	*48h*	*72h*	*96h*
Serum	Sigma	$9.00x10^4$	$3.48x10^5$	$1.57x10^6$	$2.40x10^6$	$4.40x10^6$
	PAN Biotech	$9.00x10^4$	$3.10x10^5$	$1.74x10^6$	$2.00x10^6$	$2.64x10^6$
	BioWest	$9.00x10^4$	$6.30x10^5$	$1.89x10^6$	$2.08x10^6$	$4.16x10^6$
	HyClone	$9.00x10^4$	$4.30x10^5$	$1.35x10^6$	$2.52x10^6$	$4.50x10^6$
	Gibco	$9.00x10^4$	$4.50x10^5$	$1.46x10^6$	$3.04x10^6$	$4.60x10^6$
	Sigma (from Marseille)	$9.00x10^4$	$4.35x10^5$	$1.01x10^6$	$2.60x10^6$	$5.00x10^6$

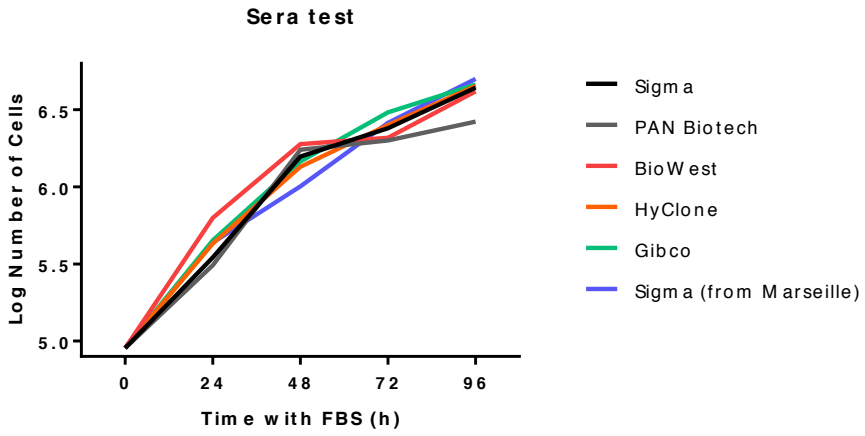

Figure 2- *Growth curve for cells grown in medium supplemented with different sera. Live cells were counted after diluting in trypan blue for each time point indicated.*

Overall, cell growth did not suffer major changes with the different sera, even though there were some small differences. After 24h and 48h of culture, the BioWest FBS was the one that promoted highest cell growth but the same pattern was not seen after 72h and 96h in culture. After 72h of culture, the serum from Gibco promoted a slightly higher growth. Also, after 96h of stimulation, there was a decrease on the cell number upon culture with the serum from PAN Biotech.

We next evaluated cell viability at the same time points by Flow Cytometry, upon Propidium Iodide staining. Graphs with the gating strategy can be seen as an example on Figure 3. The resultant percentage of viable cells can be seen on Table 5.

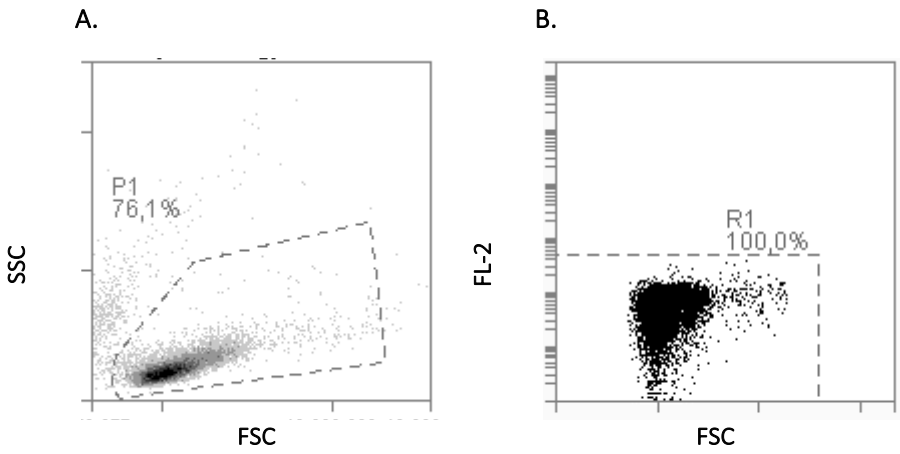

Figure 3 – *Flow Cytometry analysis of cell viability for CAL-1 cells.* ***A*** *–selection of the area containing events considered for analysis of cell viability (gating – P1 region);* ***B*** *– viable cells will not stain for propidium iodide and thus are located in the gated area (R1).*

Table 5 - *Percentage of viable cells for each serum and in each time point. The percentage was obtained by Flow Cytometry analysis upon Propidium Iodide staining.*

	0h	*24h*	*48h*	*72h*	*96h*
Sigma	100%	99.9%	99.8%	98.1%	98.9%
PANBiotech	100%	100%	99.8%	98.3%	99.5%
BioWest	100%	100%	99.8%	97.9%	97.9%
HyClone	100%	99.9%	99.8%	98.2%	99.2%
Gibco	100%	99.9%	99.8%	99.7%	99.6%
Sigma (from Marseille)	100%	99.9%	99.9%	99.7%	99.8%

All sera promoted good cell viability, with the percentage of viable cells being above 97% for all time points analyzed. Since the prospective work consists in the stimulation of CAL-1 cells, the expression level of cytokines is another condition to consider in order to choose a serum batch.

After CAL-1 stimulation with 3µM CpG-A, expression of IFN-α, IFN-β and TNF-α mRNA was measured by RT-qPCR at different time-points (3h, 6h and 9h) comparing to the control (0h) (Figure 4). These cytokines were used, since their expression is known to be promoted by CpG-A stimulation (73).

A.

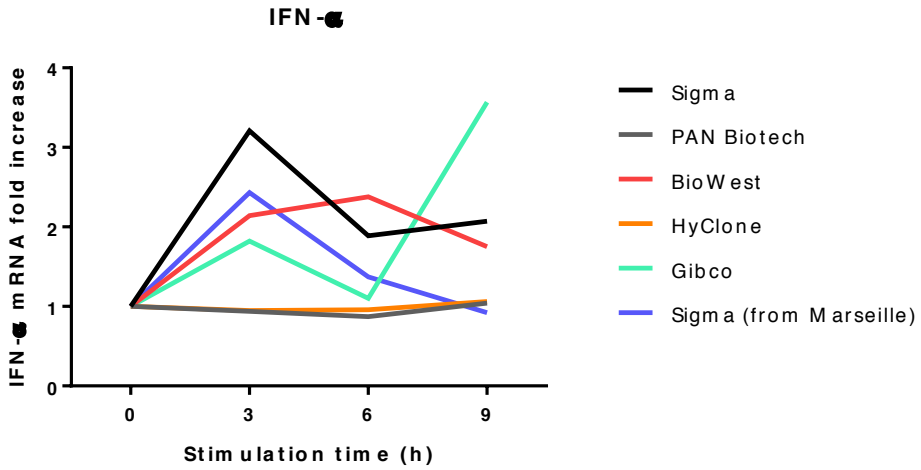

B.

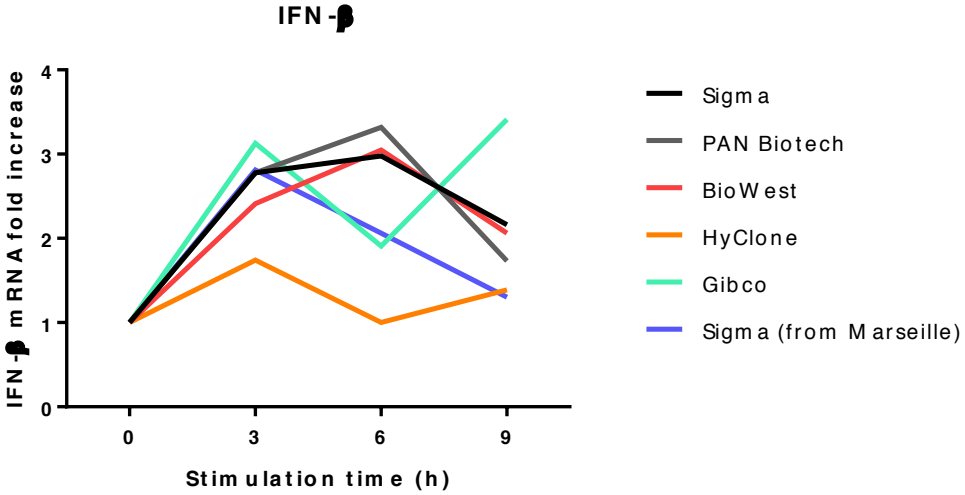

C.

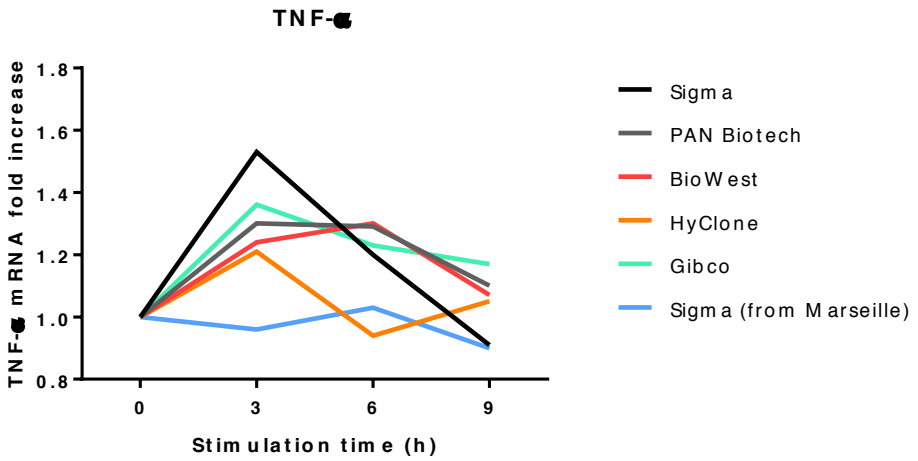

Figure 4 – Expression of mRNA for IFN-α (A), IFN-β (B) and TNF-α (C) was determined by RT-qPCR for CAL-1 cells cultured in medium supplemented with different batches of serum and stimulated with CpG-A. GAPDH was used as a reference gene and mRNA expression was normalized against values obtained for 0 h of incubation.

In general, all sera batch promoted an increased expression of cytokine mRNA between 3-6h upon stimulation. The HyClone serum led to a low expression of cytokines and thus it was no longer considered. The Gibco serum was also excluded due to the abrupt decrease in cytokines level after 6h and abrupt increase after 9h of stimulation, showing an irregular pattern over time. Looking at the tendency on Figure 4-A, the serum with improved expression of IFN-α after 3h of stimulation of CpG-A was the Sigma serum. After 6h of stimulation, the BioWest serum showed the highest production of IFN-α, followed by Sigma. After 9h, it was again the batch from Sigma that promoted more IFN-α production. Observing Figure 4-B, after 3h of stimulation both PANBiotech and Sigma sera showed the highest expression of IFN-β. However, after 9h the Sigma serum led to a diminished expression of IFN-β. Finally, looking at Figure 4-C, even though expression of TNF-α mRNA remained very low, the batch from Sigma promoted higher expression of TNF-α 3h after stimulation, followed by a decrease at 6h and 9h post-stimulation.

Thus, every serum batch promoted a good growth tendency but the sera that seems to be more efficient to study the activation pattern of CAL-1 cell is the one from Sigma. All subsequent assays were performed with this batch.

Optimizing LL37 Concentration for CAL-1 stimulation with immune complexes

Our goal is to analyze stimulation of CAL-1 cells with immune complexes formed with self-DNA conjugated with the LL37 peptide. However, there was no optimized concentration of LL37 to form these complexes. Therefore, we started by testing different concentrations of LL37, based on earlier pDC studies. Lande et al. 2007 evaluated IFN-α production upon stimulation with IC formed by DNA and LL37 in four different concentrations (0.3μM, 1μM, 3μM and 10μM) in primary cells. In their assays, the lower concentration of the peptide had no effect on IFN-α production. Thus, we selected four conditions to test, namely ICs formed with 5, 10, 20 and 50μg/ml, corresponding to the concentrations of 1, 2, 4 and 10μM, respectively. Firstly, CAL-1 cell viability was measured by Flow Cytometry upon stimulation with immune complexes prepared with these different concentrations for 6h and 24h (Figures 5 and 6). The gating strategy adopted was similarly to the one previously described (Figure 2-A).

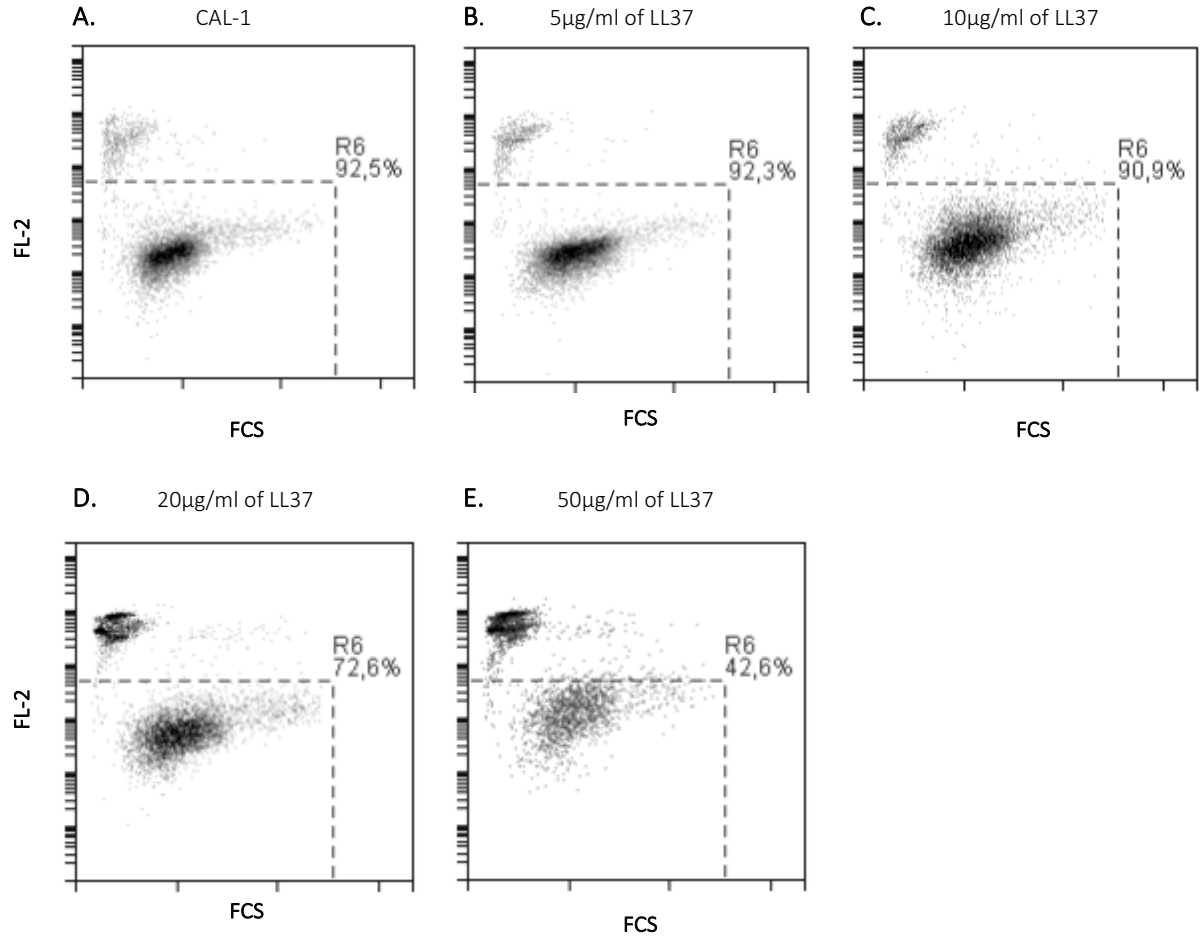

Figure 5 – *Evaluation by Flow Cytometry of CAL-1 cells viability after 6h of stimulation with IC with different concentrations of LL37. Plots show the intensity of Propidium iodide staining (FL2) against FCS. The percentage of events (R6) represents the viable cells. A – cells with no treatment; B – cells treated with IC prepared with 5μg/ml of LL37; C – cells treated with IC*

prepared with 10µg/ml of LL37; D – cells treated with IC prepared with 20µg/ml of LL37; E – cells treated with IC prepared with 50µg/ml of LL37.

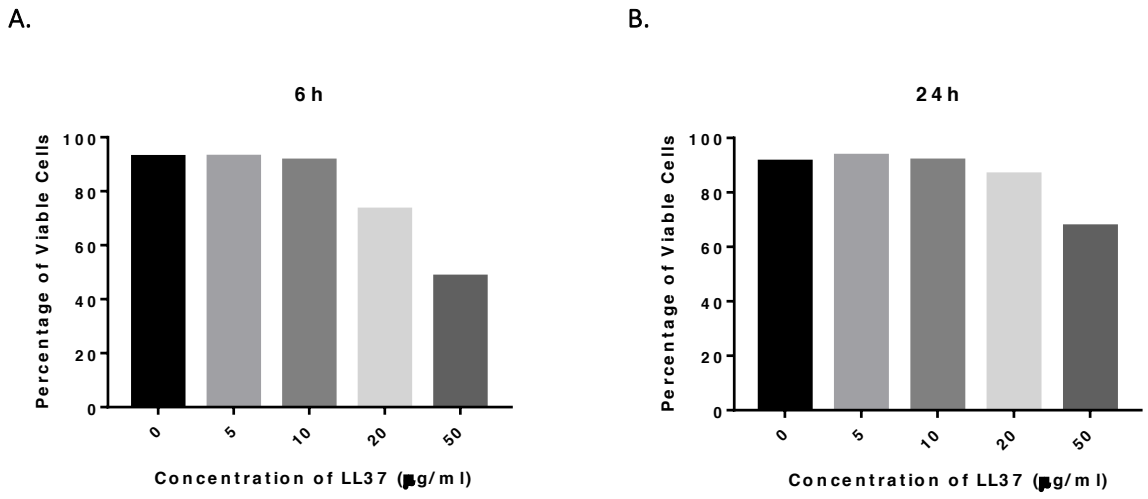

Figure 6 *– Percentage of viable cells after 6h (A) and 24h (B) of incubation with immune complexes prepared with different LL37 concentrations (5, 10, 20 and 50µg/ml). Data was obtained by Flow Cytometry upon Propidium Iodide staining.*

After 6h of incubation, the control condition (CAL-1 cells alone – Figure 5-A) shows a percentage of viable cells close to 90%, indicating some cellular death, as expected. This cellular death increased when CAL-1 cells were stimulated with the IC containing 20µg/ml of LL37 and even more so for 50µg/ml. However, lower concentrations of LL37 in the complexes allowed for a higher percentage of viable cells, with similar levels to the control conditions. This is in agreement with previous results where higher concentrations of LL37 peptide decreased the percentage of viable cells in neutrophils (108). However, in their studies, Zhang et al., 2008 found that this cell death induction is clearly evident only when doses exceed 5µM. This may not be true for pDCs/CAL-1 cells, since cellular death seems to be enhanced in doses higher than 4µM (20µg/ml).

We next evaluated which concentration of LL37 peptide is best to form ICs that activate CAL-1. For that, we quantified expression of mRNA for the cytokines IFN-α, IFN-β and TNF-α by RT-qPCR upon 6h of CAL-1 stimulation with immune complexes formed with different concentrations of LL37 (Table 6 and Figure 8). Cytokine expression was also evaluated for the conditions with 24h of incubation. Nevertheless, no expression was detected, since cytokine mRNA is generally not detected after 24h, as can be seen on earlier results, which showed a reduction after 9h stimulation.

Table 6 - *Relative amount of IFN-α, IFN-β and TNF-α mRNA expressed by CAL-1 stimulated with the complexes formed with the indicated amount of LL37, measured by RT-qPCR, after 6h of incubation.*

		CAL-1 alone	*DNA alone*	*50µg/ml of LL37*	*20µg/ml of LL37*	*10µg/ml of LL37*	*5µg/ml of LL37*	*CpG*
IFN-α	1st test	-	1	2.203	0.798	2.605	3.577	1.207
	2nd test	1	2.269	20.225	0.069	4.834	2.569	2.527
	3rd test	1	0.303	0.208	0.298	0.265	0.476	1.2
	4th test	1	0.137	0.149	0.074	544.284	0.512	283.432
	5th test	1	0.310	6.185	0.459	0.51	0.437	1.939
IFN-β	1st test	-	1	2.203	0.849	2.335	3.053	0.826
	2nd test	1	1.666	11.316	0.055	3.844	1.629	1.648
	3rd test	1	0.287	0.180	0.371	0.389	0.391	1.430
	4th test	1	0.809	0.048	1.179	8932.565	1.299	52.101
	5th test	1	1.278	1.442	0.352	0.362	0.531	2.351
TNF-α	1st test	-	1	0.869	1.372	1.015	1.414	1.731
	2nd test	1	0.953	0.808	1.04	0.665	0.642	0.711
	3rd test	1	0.296	0.23	0.32	0.245	0.161	1.116
	4th test	1	0.619	0.437	0.937	131.077	0.069	342.528
	5th test	1	0.386	0.394	0.1	0.301	0.357	1.009

At the fourth test, values were extremely high for all cytokines (in red) for the condition containing 10µg/ml of LL37 (Table 6), suggesting that some contamination might have occurred, which resulted in an outlier. Excluding these values from further analysis, some variability still remains visible. Indeed, error bars were very high, which was not expected since we were working with a cell line. The variability between assays may have been caused by the reduced shelf-life of the LL37 peptide (one month) or even the passage of cells on each experiment, which varied from 7 to 23. Thus, these assays should be repeated to have more coherent data. At these stage, no statistically significant differences have been detected. Nevertheless, some tendencies were evident. In general, the immune complexes with 50µg/ml of LL37 peptide promoted higher expression of IFN-α, IFN-β and a lower expression of TNF-α (Figure 7). However, as shown earlier, this concentration decreased cell viability (Figure 5). Immune complexes with 10µg/ml of LL37 also promoted higher expression of IFN-α, IFN-β and a lower expression of TNF-α, even though at lower levels. The immune complexes with 20µg/ml of LL37 decrease the expression of IFN-α, IFN-β, being even lower than CAL-1 cells alone, and increase slightly the expression of TNF-α, reversing the effect of the other concentrations. CAL-1 cells stimulated only with self-DNA seem to have basal expression of all cytokines, similarto unstimulated CAL-1 cells. In contrast to IFNs, TNF-α mRNA expression remained very low for all conditions. This data is not unexpected given that Ganguly et al., 2009 showed that pDCs are able to

induce IFN-α but not TNF-α. Also, the similarity between IFN-α and IFN-β expression is not surprising, since the same receptor (IFNAR1) is necessary for induction of both (63,64). Comparing CAL-1 cells alone with the positive control (CpG-A), cells incubated with CpG-A enhance IFN-α and IFN-β mRNA expression, similar to Steinhagen et al., 2012 where CAL-1 cells and primary human pDCs stimulated with CpG-A showed a similar behavior. Additionally, they also showed that CpG-A stimulation does not induce TNF-α mRNA expression, in agreement with our results.

A.

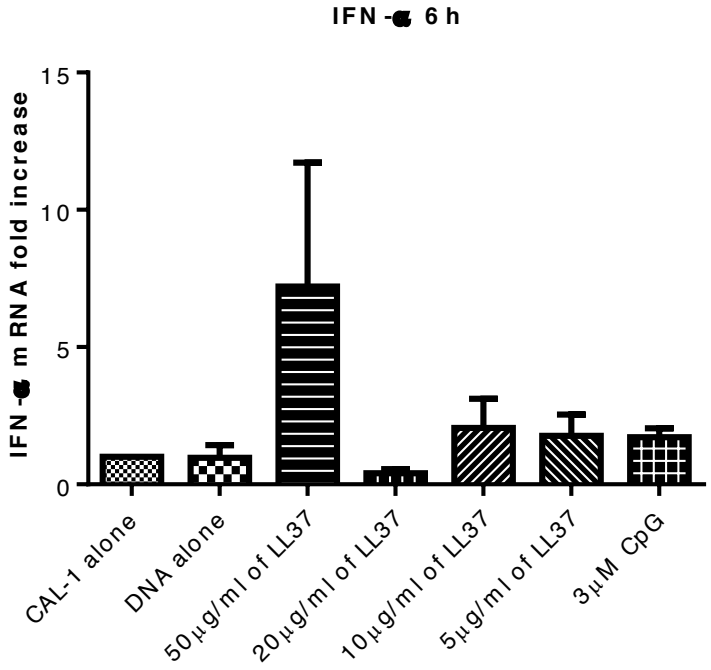

B.

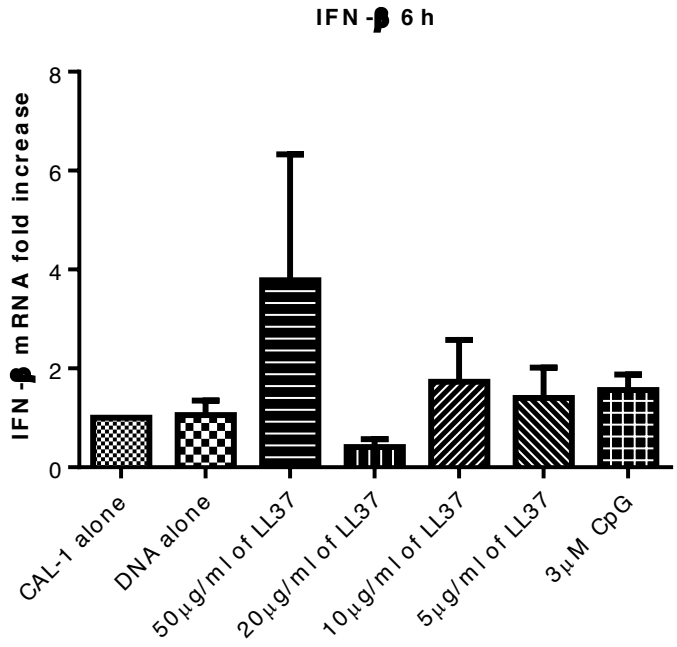

C.

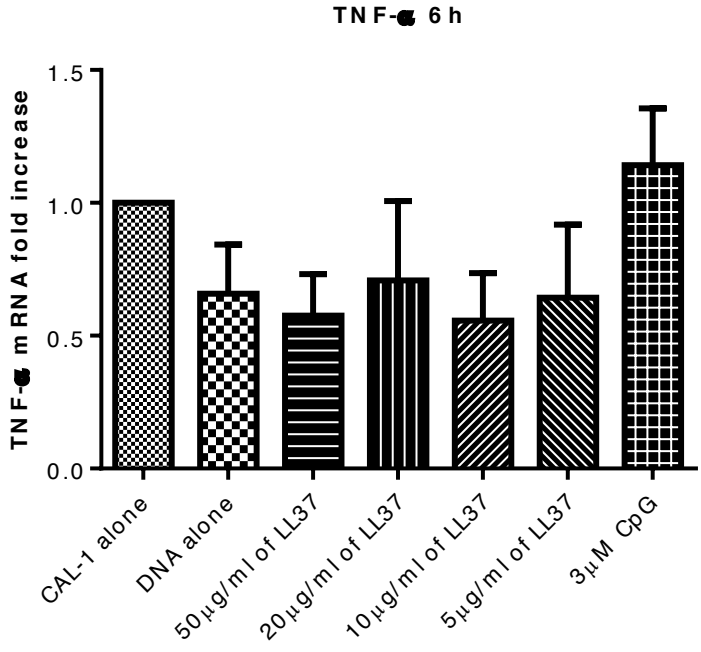

Figure 7 – *Expression of mRNA for IFN-α (A), IFN-β (B) and TNF-α (C) was determined by RT-qPCR for CAL-1 cells incubated with immune complexes prepared with different LL37 concentrations (5, 10, 20 and 50µg/ml) and stimulated in parallel with CpG-A or with self-DNA, as controls. GAPDH was used as a reference gene and mRNA expression was normalized against values obtained for 0 h of incubation. Data are mean of four independent experiments, error bars represent the SEM.*

Overall, since using of 50µg/ml of LL37 led to a decrease on cell viability of about 50%, the concentration more efficient to study activation of CAL-1 cell is 10µg/ml of LL37.

To analyze which concentration of LL37 peptide is best to induce cytokine production, we further evaluated protein secretion for the cytokines IFN-α, TNF-α and IL-1β by ELISA (Figure 8). However, no secretion of IFN-α and TNF-α was detected. IFN-α absence is contradictory to our early results. These data are inconsistent with Ganguly et al., 2009 and Steinhagen et al., 2012 studies, where they show IFN-α and TNF-α secretion upon stimulation for 4h of pDCs with immune complexes in primary cells, or stimulation for 3h of CAL-1 cells with CpG-A, respectively. Supernatants for 6h incubation were also tested, although no secretion was detected.

CAL-1 cells stimulated only with self-DNA showed the highest production of IL-1β. Then, the second highest production of IL-1β is due to CpG-A stimulation, followed by the ICs with 10µg/ml of LL37. In addition, all the other tested concentrations promoted a lower secretion of IL-1β.

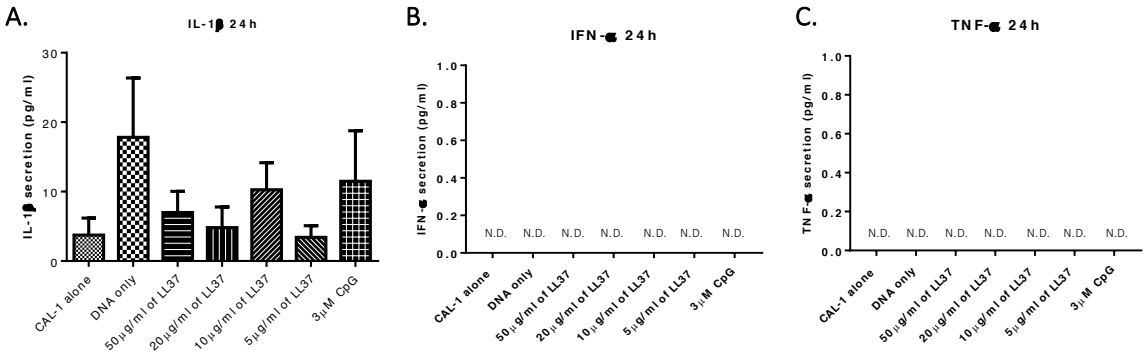

Figure 8 *– Protein secretion determined by ELISA for CAL-1 cells incubated with immune complexes prepared with different LL37 concentrations (5, 10, 20 and 50µg/ml) and stimulated in parallel with CpG-A and only with self-DNA. A – IL-1β secretion; B – IFN-α secretion; C - TNF-α secretion Data are mean of five independent experiments, error bars represent the SEM.*

There are currently no publications regarding the induction of inflammasomes, detected by IL-1β secretion, on CAL-1 cells pDCs. However, Dombrowski and Schamber et al., 2012 refer that the LL37 peptide inhibits the AIM2 (cytosolic receptor that forms an inflammasome after sensing cytosolic dsDNA) inflammasome activation in keratinocytes in psoriasis by neutralizing cytosolic self-DNA, thereby blocking IL-1β release. On Figure 8, it is clear that CAL-1 cells incubated only with self-nDNA promoted the highest IL-1β secretion. When dsDNA was conjugated with LL37, IL-1β secretion decreased. Thus, our study also provides some evidence of inhibition of inflammasome on CAL-1 cells, although more tests are required. Consequently, beyond being the best to induce type I IFNs

mRNA expression, the immune complexes of LL37 with selfDNA seem also to modulate IL-1β secretion. In future work it will be interesting to also measure IL-1β mRNA expression by RT-qPCR.

Taken together, these data suggest that, the concentration of LL37 promoting CAL-1 cells activation, is 10µg/ml. However, for immune complexes no ideal nDNA concentration is known for our cells.

Optimizing DNA Concentration for CAL-1 stimulation with immune complexes

To achieve our goal of analyze stimulation of CAL-1 cells with immune complexes formed with self-DNA conjugated with the LL37 peptide, there is a need to also optimize the concentration of DNA to form these complexes. Therefore, we started by testing different concentrations of DNA, based on earlier pDC studies. In their studies, Lande et al., 2007, tested CAL-1 cells using DNA at concentrations of 0.1, 0.5, 2 and 10 µg/ml. Ganguly et al., 2009 showed that 1µg/ml is enough to promote a good pDC activation. Here, some different concentrations of self-nuclear DNA (nDNA) were chosen to form ICs and stimulate CAL-1 cells: 1µg/ml, 0.5 µg/ml and 0.2 µg/ml.

Thus, mRNA expression for IFN-α, IFN-β and TNF-α was measured by RT-qPCR, upon stimulation with immune complexes prepared with these different concentrations. Five assays were performed upon stimulation for 6h and 24h (Table 7 and Figure 9).

Table 7 - *Relative amount of IFN-α, IFN-β and TNF-α mRNA expressed by CAL-1 stimulated with the complexes formed with the indicated amount of nDNA, measured by RT-qPCR, after 6h of incubation.*

		CAL-1 alone	*nDNA alone*	*LL37 alone*	*CpG-A*	*1µg/ml of nDNA*	*0.5µg/ml of nDNA*	*0.2µg/ml of nDNA*
IFN-α	*1st test*	1	0.8	0	59.743	3.544	0.095	1.225
	2nd test	1	9.049	2.342	10.31	5.679	7.992	11.846
	3rd test	1	2.989	5.162	0.531	1.486	2.457	0.074
	4th test	1	2.027	0.719	1653.929	0.109	0.045	0.017
	5th test	1	0.912	0.45	1.356	0.372	0.294	1.291

IFN-β	*1st test*	1	2.185	0	490.053	1.368	0.531	1.368
	2nd test	1	9.184	3.784	29.281	6.177	14.99	9.469
	3rd test	1	0.898	23.83	0.34	0.278	0.793	0.046
	4th test	1	0.255	3.39	974.032	0.015	0.001	0.006
	5th test	1	0.87	0.607	1.246	0.851	0.585	1.737
TNF-α	*1st test*	1	1.142	0.774	2.016	0.886	0.872	0.96
	2nd test	1	1.595	3.714	2.965	2.147	2.085	1.988
	3rd test	1	1.274	1.474	1.002	0.971	1.424	0.559
	4th test	1	3.55	0.123	6505.287	0.036	0.007	0.123
	5th test	1	0	0.863	1.569	1.079	0.556	0.965

As before, there was excessive expression of each cytokine at the fourth test, and also at the first test for IFN-β (in red) (Table 7), suggesting some contamination. Excluding these values, some variability remains visible. Again, we found no statistically significant differences but some tendencies were evident. In general, all the cytokines show less mRNA than the positive control, CpG-A (Figure 10). For IFN-α, the immune complexes formed with 0.2µg/ml of DNA lead to higher levels of mRNA than the other concentrations. Also for IFN-α, CAL-1 cells stimulated only with self-DNA, show higher mRNA expression than CAL-1 cells alone. For TNF- α, values remained very low, and CAL-1 cells stimulated only with LL37, showed higher mRNA expression than CAL-1 cells alone. In theirs studies, Zhang et al., 2008 showed that LL37 may somehow link with some hypothetical self-DNA extruded from the cell (108). However, for cells stimulates only with self-DNA, this link can not be seen since LL37 is only expressed in injured cells (48). Overall, the levels of mRNA obtained upon stimulation with immune complexes remained low and there were no statistically significant differences compared with the control. Thus, despite the immune complexes formed with 0.2µg/ml of DNA express more IFN-α mRNA, no ideal concentration of nDNA can be chosen.

A.

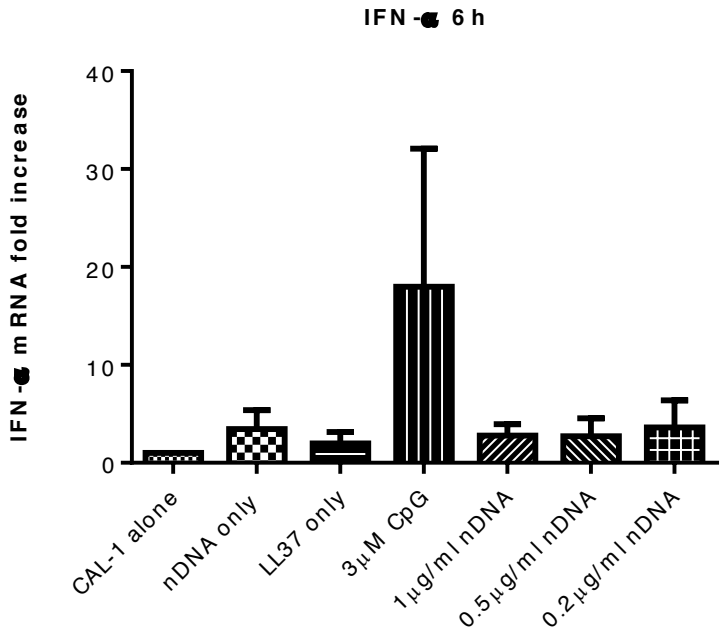
IFN-α 6 h
IFN-α mRNA fold increase
40
30
20
10
0
CAL-1 alone
nDNA only
LL37 only
3μM CpG
1μg/ml nDNA
0.5μg/ml nDNA
0.2μg/ml nDNA

B.

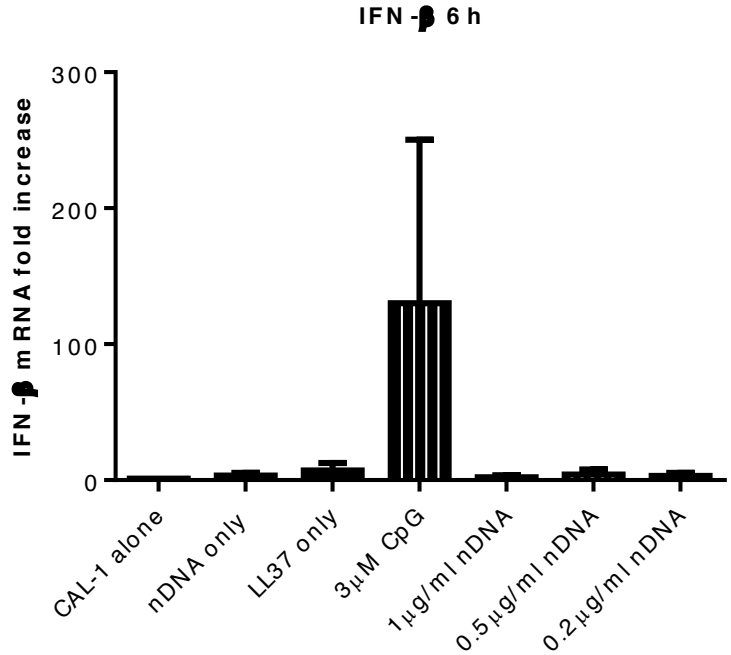
IFN-β 6 h
IFN-β mRNA fold increase
300
200
100
0
CAL-1 alone
nDNA only
LL37 only
3μM CpG
1μg/ml nDNA
0.5μg/ml nDNA
0.2μg/ml nDNA

C.

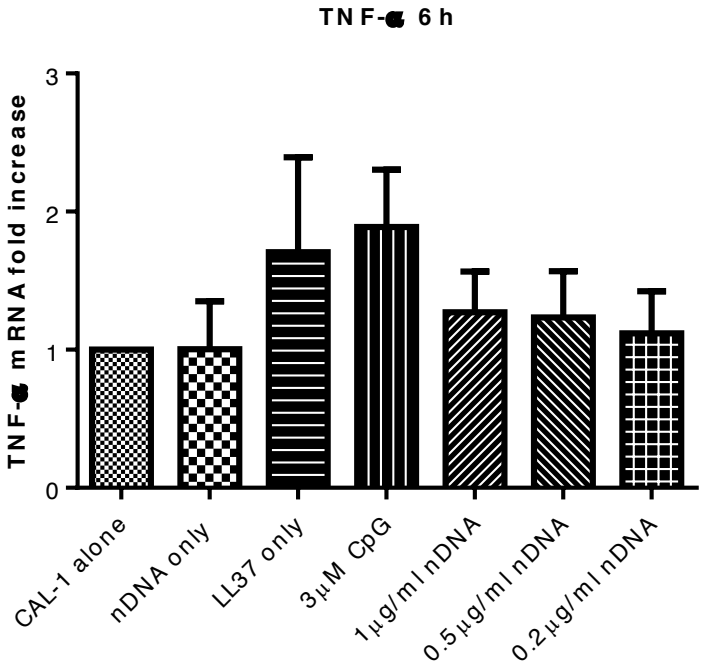

Figure 9 *- Expression of mRNA for IFN-α (A), IFN-β (B) and TNF-α (C) was determined by RT-qPCR for CAL-1 cells incubated with immune complexes prepared with different nDNA concentrations (1, 0.5 and 0.2μg/ml) and stimulated in parallel with CpG-A and only with LL37 and self-DNA. GAPDH was used as a reference gene and mRNA expression was normalized against values obtained for 0 h of incubation. Data are mean of four independent experiments, error bars represent the SEM.*

In addition to nDNA, mitochondrial DNA (mtDNA) might also be able to activate pDCs. The formation of either the nDNA or mtDNA complexes are thought to play a similar role in pDC activation (53). To test this fact, an analysis of the immune complexes formed by LL37 peptide with mtDNA was made. However, the quantity of mtDNA obtained in the extraction from CAL-1 cells was always very low, making it difficult to repeat the assay and optimize mtDNA concentration. Thus, some alternative method of mtDNA isolation should be tested to obtain better results, such as a mtDNA isolation kit (53).

Nevertheless, we evaluated mRNA expression of IFN-α, IFN-β and TNF-α by RT-qPCR, upon stimulation with immune complexes prepared with 0.5μg/ml of self-mtDNA. Two assays were performed upon stimulation for 6h (Table 8 and Figure 10).

Table 8 – *Relative amount of IFN-α, IFN-β and TNF-α mRNA expressed by CAL-1 stimulated with the complexes formed with the indicated amount of mtDNA, measured by RT-qPCR, after 6h of incubation.*

		Cells	*mtDNA only*	*LL37 only*	*CpG-A*	*0.5µg of mtDNA*
IFN-α	*1st test*	1	3.286	0	59.743	7332.045
	2nd test	1	9.207	0	10.31	7.698
IFN-β	*1st test*	1	4.25	0	490.053	795774.421
	2nd test	1	9.388	0	29.281	6.065
TNF-α	*1st test*	1	0.904	0.774	2.016	2123.164
	2nd test	1	3.002	0	2.965	3.055

The expression of cytokines mRNA shows a huge variability. In general, CAL-1 cells stimulated only with self-mtDNA alone, CpG-A and the immune complexes showed more mRNA expression than CAL-1 cells alone. Stimulation with LL37 alone caused almost no expression, as expected, despite being inconsistent with previous results. In addition, a clear effect of the immune complexes with mtDNA and LL37 can be seen on CAL-1 cells stimulation. For this condition, mRNA expression was higher for type I than for TNF-α. This is similar to earlier results for LL37 and nDNA optimization assays and to the work of Lande et al., 2007, suggesting that pDCs express higher levels of IFN-α and IFN-β mRNA than TNF-α. Comparing with earlier results, CAL-1 cells stimulation with immune complexes with LL37-mtDNA promoted higher expression of cytokines than stimulation with LL37-nDNA immune complexes. This is in agreement with the work published by as Zhang et al. 2015 on pDCs, showing that LL37-mtDNA complexes exacerbate inflammation and stimulate IFN-α production, comparing to LL37-nDNA complexes (53,54).

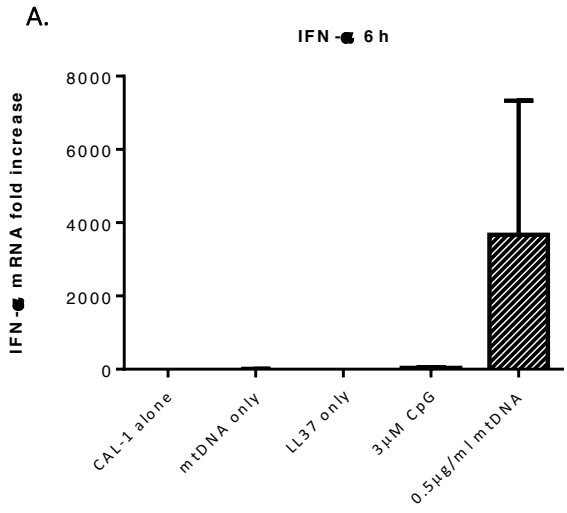

B.

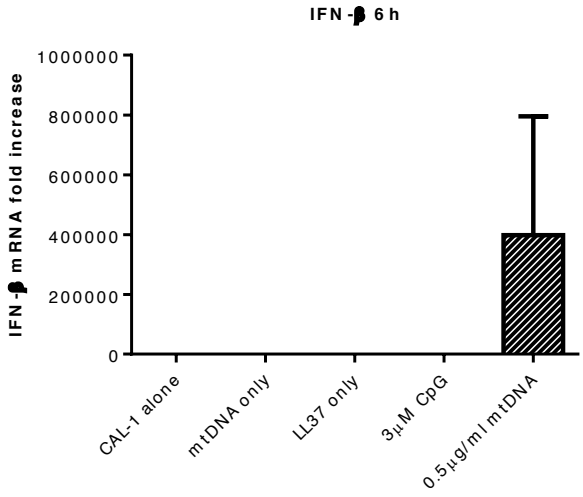

C.

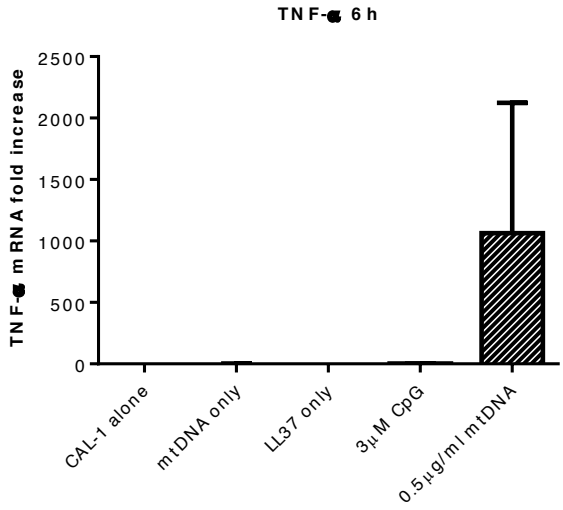

Figure 10 - *Expression of mRNA for IFN-α (A), IFN-β (B) and TNF-α (C) was determined by RT-qPCR for CAL-1 cells incubated with immune complexes prepared with a concentration of 0.5μg/ml of mtDNA and stimulated in parallel with CpG-A and only with LL37 and self-mtDNA. GAPDH was used as a reference gene and mRNA expression was normalized against values obtained for 0 h of incubation. Data are mean of four independent experiments, error bars represent the SEM.*

Finally, secretion of IFN-α, TNF-α and IL-1β was measured by ELISA assays. Five assays were performed upon stimulation for 6h and 24h (Figure 11). Again, no secretion of IFN- α and TNF-α was detected, as seen earlier.

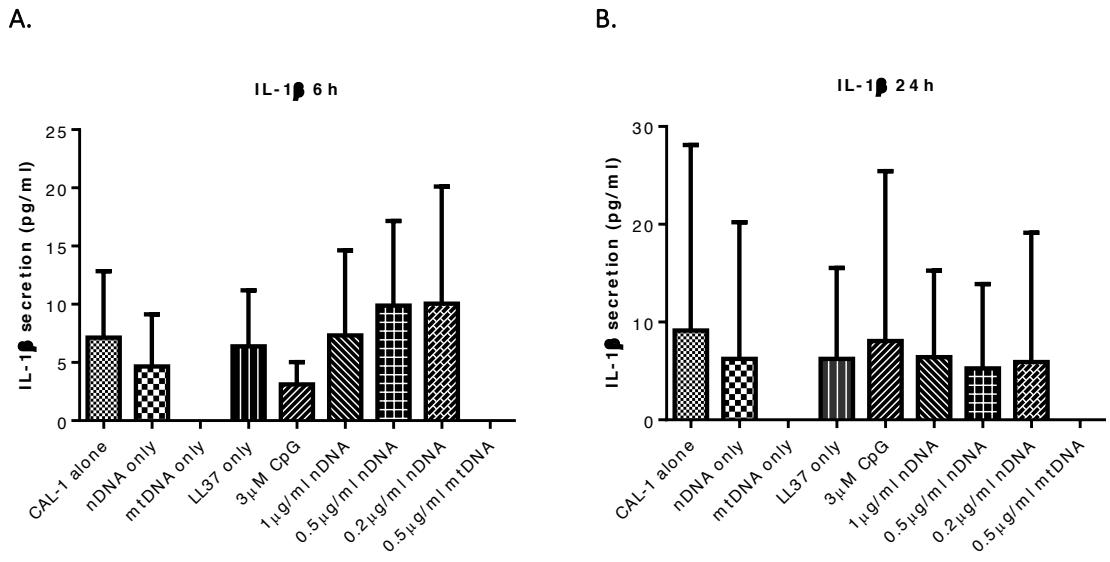

Figure 11 - *Secretion of IL-1ß determined by ELISA for CAL-1 cells incubated for 6h (A) and 24h (B) with immune complexes prepared with different nDNA concentrations (1, 0.5, 0.2µg/ml) and mtDNA (0.5µg/ml) or stimulated in parallel with CpG-A or only with LL37 and self-DNA, self-mtDNA. Data are mean of five independent experiments, error bars represent the SEM.*

Analyzing the data, the differences between the conditions are very small and the error bars are huge. Thus, all data should be repeated to obtain better results.

Interestingly, no secretion of cells stimulated with self-mtDNA alone and immune complexes of LL37-mtDNA is seen in both time-points, suggesting that mtDNA, even in complex, may not be able to induce the inflammasome formation. This is not shocking since AIM2 inflammasome activation is induced by detection of cytosolic dsDNA and mtDNA, although being dsDNA, it has a circular form, and may not be recognized by AIM2. However, no studies in this subject are known.

Analyzing all data acquired, no robust answer of the best concentration of nDNA can be found. Nevertheless, mRNA expression for IFN-α and IL-1β was generally higher when CAL-1 cells were stimulated with immune complexes with 0.2µg/ml of nDNA, appearing to be the best nDNA concentration to form immune complexes and activate CAL-1 cells. However, more data are needed to have a consistent result. Also, the error bars are, again, too high, not being expected since we were working with a cell line. Furthermore, the variability between the assays led to a huge standard deviation, increasing the error bar. Thus, these assays should be repeated to obtain more coherent data.

Co-localization Analysis by IF

After choosing the best concentrations of LL37 peptide and self-nDNA to form immune complexes to activate CAL-1 cells, we started exploring how and how long it takes to the immune complexes to enter the cell, recruit the early endosomes and trigger the TLR-9 signaling pathway. For that, we performed an immunocytochemistry analysis of stimulated cells, by staining for LL37, endosomes and TLR-9. We first compared the control conditions (CAL-1 cells alone, CAL-1 stimulated with CpG-A, CAL-1 stimulated with LL37 alone and CAL-1 stimulated with DNA alone) to understand whether CAL-1 cells activation may affect expression of TLR-9 and induction of early endosomes (EEA1) (Figure 12). LL37 peptide was stained with Mouse anti-LL37-Alexa-Fluor-488, the early endosomes, stained with Rabbit anti-EEA1 with the secondary Alexa-Fluor-647 and the TLR-9 receptor stained with Mouse anti-TLR-9 with the secondary Alexa-Fluor-568. One assay was performed for each time-point.

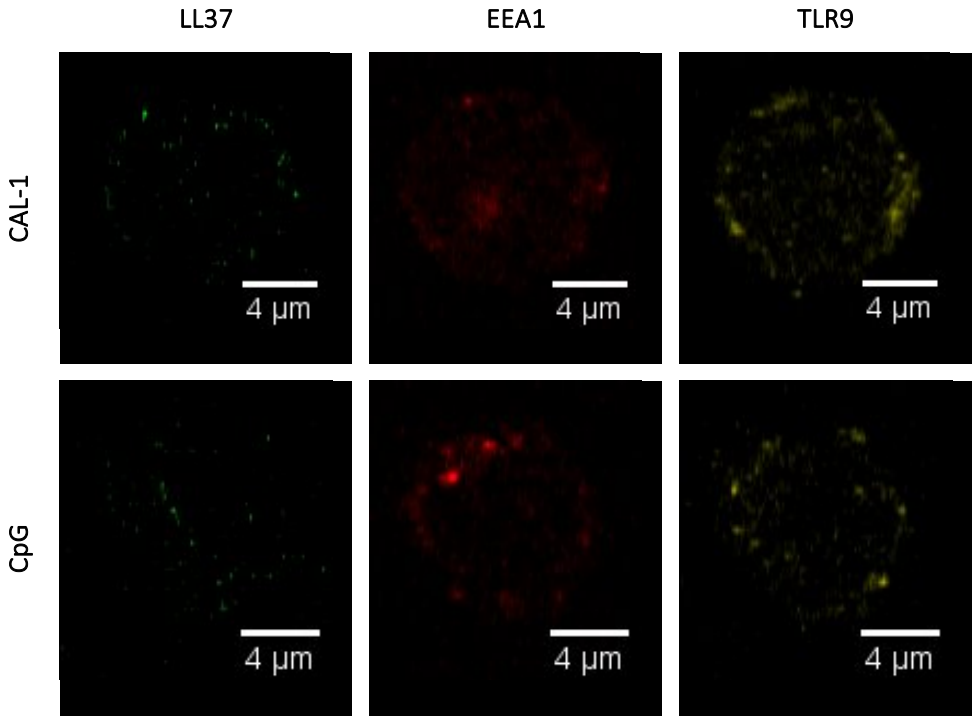

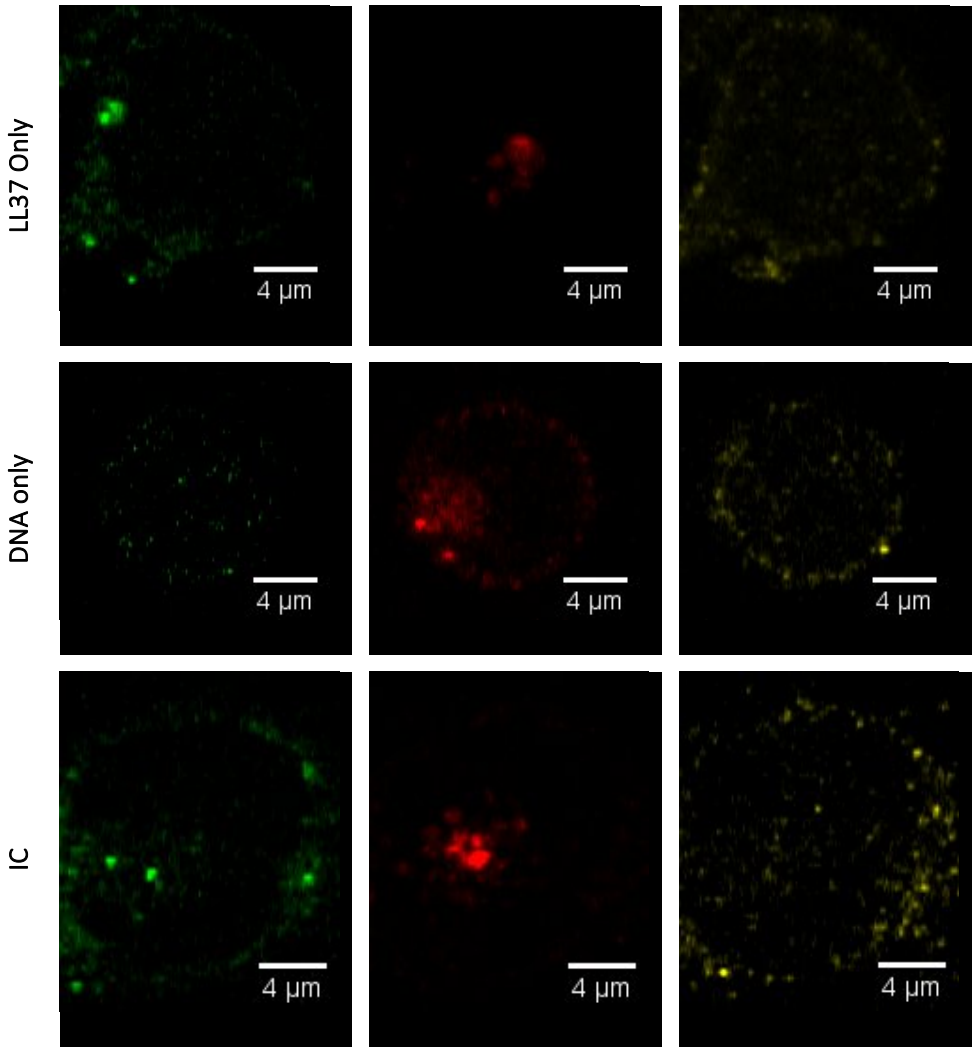

Figure 12 – *Immunofluorescence microscopy analysis showing the staining of, TLR-9, early endosomes (EEA1) and LL37 in the control conditions: CAL-1 cells alone, CAL-1 cells stimulated with CpG-A, CAL-1 cells stimulated only with LL37 and CAL-1 cells stimulated only with self-nDNA, at 120minutes of incubation. Scale bars = 4µm. Images are representative of CAL-1 cells, in mean 9 cells per condition.*

As expected, CAL-1 cells alone and CAL-1 stimulated with CpG-A or with DNA alone did not stain for LL37, thus confirming that the LL37 peptide is not expressed on normal conditions, as stated by Lande et al., 2007. Early endosomes were present in all conditions, although some differences were visible: first, for CAL-1 cells alone staining was lower that for all the remaining conditions, and second, early endosomes are surrounding the cells near the membrane in all conditions, expect for those that contain LL37 peptide, where a round shape staining was visible near one side of the cell. TLR-9 triggering seemed to enhance upon activation by CpG-A, as in Combes et al., 2017, and with ICs, and also surprisingly by cells stimulated with only self-DNA.

We next proceeded to perform a co-localization analysis of ICs with either TLR9 or EEA1 (early endosome marker), at different time-points (15, 30, 60 and 120minutes). Data were compared to the same conditions with 0h of incubation (Figure 13).

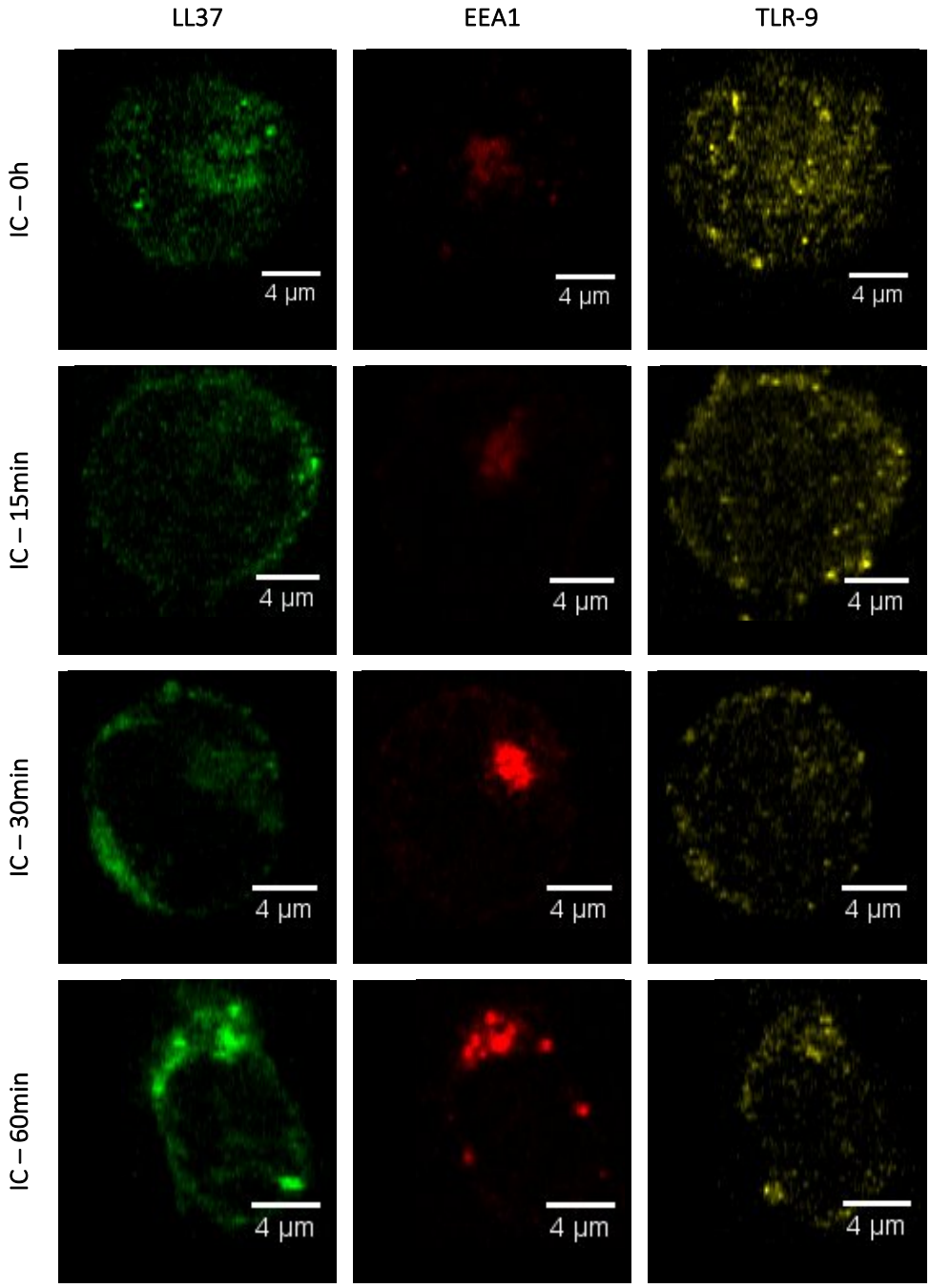

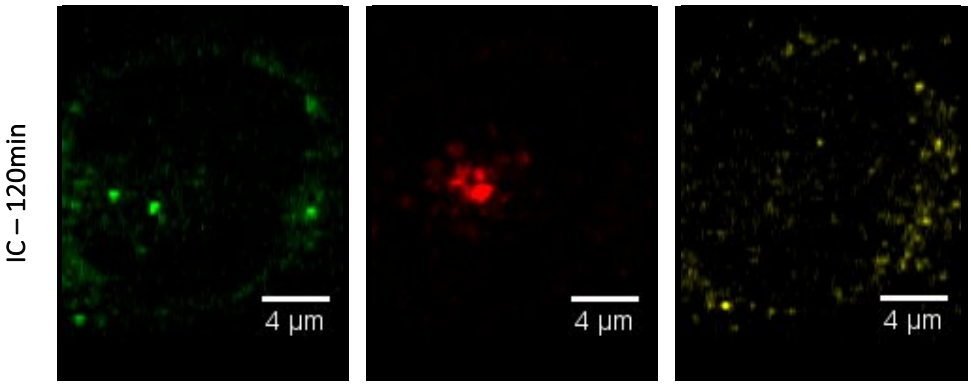

Figure 13 *– Immunofluorescence microscopy analysis to detect the presence of the immune complexes with LL37 staining and the recruitment of TLR-9 and the early endosomes (EEA1) by the immune complexes, at different time points (15, 30, 60 and 120minutes). Non-treated condition (0h) was used as a reference. Scale bars = 4µm. Images are representative of CAL-1 cells, in mean 9 cells per condition.*

It was found that LL37 peptide of the immune complexes was surrounding the cell until 60minutes of incubation while at 120min of incubation, little spots of LL37 could be seen inside the cell. This raises the possibility that the immune complexes take between 60-120minutes to enter the cell. On the other hand, early endosomes recruitment does not seem to start at the same time-point. Observing EEA1 staining, the role of early endosomes in this pathway seems to start 60minutes after the incubation with the immune complexes. TLR-9 was located near the early endosomes and co-localized with the peptide only after 60minutes of incubation with ICs.

Co-localization of the LL37 of the immune complexes with both EEA1 and TLR-9 was determined by measuring the Pearson's Coefficient for each cell in test, using the plugin JACoP, of ImageJ software, in each time-point (Figure 14).

A.

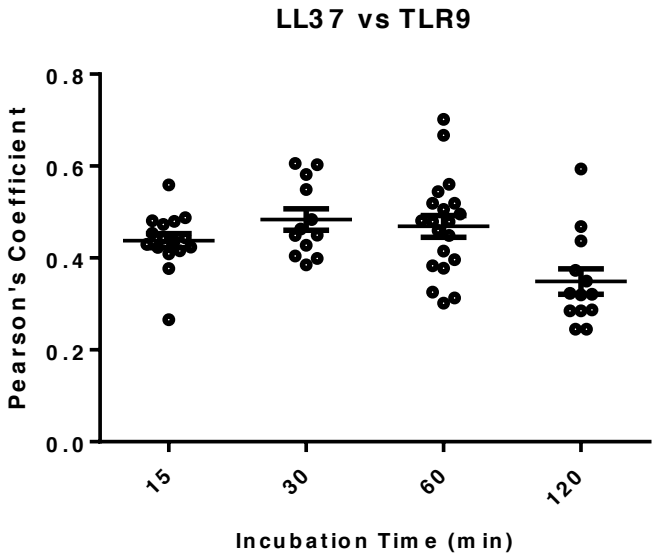

B.

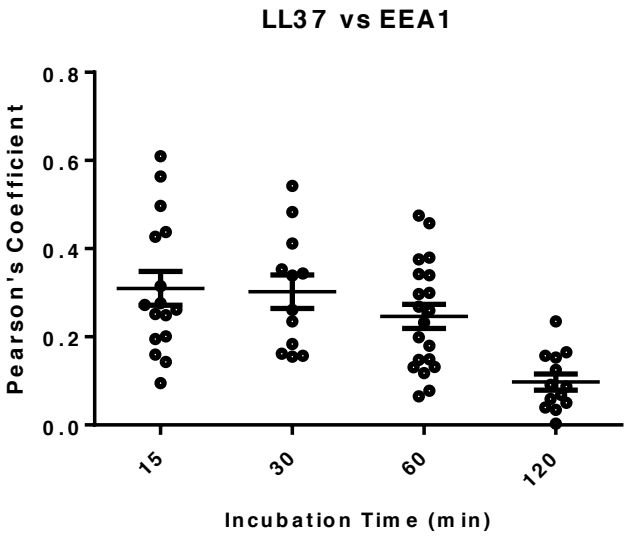

Figure 14 – *Co-localization analysis expressed by Pearson's Coefficient for LL37 and TLR-9 (A) and for LL37 and EEA1 (B), at different time-points (15, 30, 60 and 120 minutes). Data are representative of each cell (12<n<20) in each condition obtained by Immunofluorescence and Pearson's Coefficient was measured by JACoP plugin of ImageJ. Error bars represent the SEM and the middle bar represents the mean.*

In general, a heterogeneous population of cells is seen, showing different behaviors within the same condition. For LL37 and TLR-9, the best correlation is clear between 30-60minutes of incubation with the complexes. However, the cell population is more homogeneous after 60minutes of incubation, being similar to the results on Figure 13.

For LL37 and EEA1, the best correlation is saw between 15-30minutes of incubation, thus suggesting that early endosomal recruitment begins after 15minutes of incubation with ICs. However, for 15minutes, the cell population is extremely heterogeneous, being more consistent between 30-60minutes of incubation. Also, TLR-9 need to be translocated to the endosomal compartment and during this translocation, they can co-localize with the immune complexes surrounding the cell, enhancing the coefficient wrongly.

Taken together, these data suggest that the internalization of the immune complexes occurs between 30-60minutes, recruiting early endosomes and triggering TLR-9 signaling. As stated earlier, upon 120minutes the coefficient decreases for both conditions (Figure 14), suggesting that 2h after adding the complexes, these have been processed and no longer remain associated with early endosomes nor TLR-9. Combes et al., 2017 showed that CAL-1 cells and pDCs promote TLR-9 and early endosomal recruitment upon 1h of stimulation, although the marker for endosomes was BAD-LAMP and stimulation performed with CpG-A. Interestingly, the coefficients decreases in both conditions (co-localization of LL37 with TLR-9 or EEA1) upon 120minutes of stimulation. This is not surprising since Combes et al., 2017 found that endosomal and TLR-9 recruitment decreased 2h upon stimulation.

Here, our results suggest that immune complexes trigger TLR-9 and early endosomes upon 30-60minutes of stimulation. After stimulation of 2h, ICs seemed to be excluded from early endosomes, decreasing the TLR-9 signaling. However, the data need to be repeated to obtain more information to answer this question.

IV. Conclusions

Conclusion

In this thesis, we showed that CAL-1 cells can be activated with immune complexes of self-DNA, which results on a type I IFN response. LL37, an antimicrobial peptide, could associate with self-nDNA, as well as with self-mtDNA, forming immune complexes that activate innate immune responses, thus breaking innate tolerance to self-DNA. This activation with immune complexes triggered the transcription of IFN-α and IFN-β mRNA, but not TNF-α in CAL-1 cells, as reported for primary pDCs. Preliminary data also indicates that activated CAL-1 cells can secrete IL-1β upon stimulation with immune complexes with self-nDNA, but not self-mtDNA, suggesting a role of nDNA-LL37 complexes in induction of the inflammasome in pDC. Our findings revealed that these immune complexes may induce activation of these cells through TLR-9 signaling and early endosomes recruitment.

Based on our work, future studies may be performed to show more insights about immune complexes formation, how they trigger TLR-9 signaling and how CAL-1 cells are related to inflammasome induction.

These findings contribute to establish CAL-1 cells as a pDC model that may possibly help to understand pDCs in the future.

V. Bibliography

1. Siegal FP, Kadowaki N, Shodell M, Fitzgerald-Bocarsly PA, Shah K, Ho S, et al. The Nature of the Principal Type I Interferon-Producing Cells in Human Blood. Science (80-). 1999;284(5421):1835–7.

2. Cella M, Jarrossay D, Facchetti F, Alebardi O, Nakajima H, Lanzavecchia A, et al. Plasmacytoid monocytes migrate to inflamed lymph nodes and produce large amounts of type I interferon. Nature Medicine. 1999;5(8):919–23.

3. Manickasingham S, Reis e Sousa C. Microbial and T cell-derived stimuli regulate antigen presentation by dendritic cells in vivo. J Immunol. 2000;165(9):5027–34.

4. Galicia G, Gommerman JL. Plasmacytoid dendritic cells and autoimmune inflammation. Biol Chem. 2014;395(3):335–46.

5. Gilliet M, Lande R. Antimicrobial peptides and self-DNA in autoimmune skin inflammation. Curr Opin Immunol. 2008;20(4):401–7.

6. Karrich JJ, Jachimowski LCM, Uittenbogaart CH, Blom B. The plasmacytoid dendritic cell as the Swiss army knife of the immune system: molecular regulation of its multifaceted functions. J Immunol. 2014;193(12):5772–8.

7. Young LJ, Wilson NS, Schnorrer P, Proietto A, ten Broeke T, Matsuki Y, et al. Differential MHC class II synthesis and ubiquitination confers distinct antigen-presenting properties on conventional and plasmacytoid dendritic cells. Nat Immunol. 2008;9(11):1244–52.

8. Swiecki M, Colonna M. The multifaceted biology of plasmacytoid dendritic cells. Nat Rev Immunol. 2015;15(8):471–85.

9. Pucchio T Di, Chatterjee B, Smed-sörensen A, Clayton S, Montes M, Xue Y, et al. Direct proteasome-independent cross-presentation of viral antigen by plasmacytoid dendritic cells on major histocompatibility complex class I. Nature. 2008;9(5):551–7.

10. Ishikawa F, Niiro H, Iino T, Yoshida S, Saito N, Onohara S, et al. The developmental program of human dendritic cells is operated independently of conventional myeloid and lymphoid pathways. Blood. 2007;110(10):3591–600.

11. Swiecki M, Colonna M. Unraveling the functions of plasmacytoid dendritic cells during viral

infections, autoimmunity, and tolerance. Immunol Rev. 2012;234(1):142–62.

12. Georg P, Bekeredjian-Ding I. Plasmacytoid dendritic cells control B cell-derived IL-10 production. Autoimmunity. 2012;45(8):579–83.

13. Facchetti F, Vermi W, Mason D, Colonna M. The plasmacytoid monocyte/interferon producing cells. Virchows Arch. 2003;443(6):703–17.

14. Zuniga E, McGavern D, Pruneda-Paz J, Teng C, Oldstone M. Bone marrow plasmacytoid dendritic cells can differentiate into myeloid dendritic cells upon virus infection. Nat Immunol 2004;5(12): 1227–1234.

15. Reizis B. Regulation of playmacytoid dendritic cell development. Curr Opin Immunol. 2010;22(2):206–11.

16. D'Amico A, Wu L. The Early Progenitors of Mouse Dendritic Cells and Plasmacytoid Predendritic Cells Are within the Bone Marrow Hemopoietic Precursors Expressing Flt3. J Exp Med. 2003;198(2):293–303.

17. Lande R, Gilliet M. Plasmacytoid dendritic cells: Key players in the initiation and regulation of immune responses. Ann N Y Acad Sci. 2010;1183:89–103.

18. Steinhagen F, Rodriguez LG, Tross D, Tewary P, Bode C, Klinman DM. IRF5 and IRF8 modulate the CAL-1 human plasmacytoid dendritic cell line response following TLR9 ligation. Eur J Immunol. 2016;46(3):647–55.

19. Rodrigues C, Cabrini M, Lenicov F, Sabatté J, Ceballos A, Jancic C, et al. Epithelial cells activate plasmacytoid dendritic cells improving their anti-HIV activity. PLoS One. 2011;6(12).

20. Chistiakov DA, Sobenin IA, Orekhov AN, Bobryshev Y V. Myeloid dendritic cells: Development, functions, and role in atherosclerotic inflammation. Immunobiology. 2015;220(6):833–44.

21. Segura E, Valladeau-Guilemond J, Donnadieu M-H, Sastre-Garau X, Soumelis V, Amigorena S. Characterization of resident and migratory dendritic cells in human lymph nodes. J Exp Med. 2012;209(4):653–60.

22. Kohara H, Omatsu Y, Sugiyama T, Noda M, Fujii N, Nagasawa T. Development of plasmacytoid dendritic cells in bone marrow stromal cell niches requires CXCL12-CXCR4 chemokine

signaling. 2007;110(9):4153–60.

23. Swiecki M, Colonna M. Accumulation of pDC: roles in disease pathogenesis and targets for immunotherapy. Eur J Immunol. 2010;40(8):2094–8.

24. Guilliams M, Henri S, Tamoutounour S, Ardouin L, Schwartz-Cornil I, Dalod M, et al. From skin dendritic cells to a simplified classification of human and mouse dendritic cell subsets. Eur J Immunol. 2010;40(8):2089–94.

25. Brown KN, Barratt-Boyes SM. Surface phenotype and rapid quantification of blood dendritic cell subsets in the rhesus macaque. J Med Primatol. 2009;38(4):272–8.

26. Dzionek a, Sohma Y, Nagafune J, Cella M, Colonna M, Facchetti F, et al. BDCA-2, a novel plasmacytoid dendritic cell-specific type II C-type lectin, mediates antigen capture and is a potent inhibitor of interferon alpha/beta induction. J Exp Med. 2001;194(12):1823–34.

27. Blasius AL, Colonna M. Sampling and signaling in plasmacytoid dendritic cells: the potential roles of Siglec-H. Trends Immunol. 2006;27(6):255–60.

28. Gilliet M, Cao W, Liu Y-J. Plasmacytoid dendritic cells: sensing nucleic acids in viral infection and autoimmune diseases. Nat Rev Immunol. 2008;8(8):594–606.

29. Matsui T, Connolly JE, Michnevitz M, Chaussabel D, Yu I, Glaser C, et al. J Immunol. 2010;182(11):6815–23.

30. Defays A, David A, Gassart A De, Rigotti FDA, Wenger T, Camossetto V, et al. BAD-LAMP is a novel biomarker of nonactivated human plasmacytoid dendritic cells. Blood. 2011;118(3):1–3.

31. Villani A-C, Satija R, Reynolds G, Sarkizova S, Shekhar K, Fletcher J, et al. Single-cell RNA-seq reveals new types of human blood dendritic cells, monocytes, and progenitors. Science (80-). 2017;356(6335):eaah4573.

32. Barton GM, Kagan JC, Medzhitov R. Intracellular localization of Toll-like receptor 9 prevents recognition of self DNA but facilitates access to viral DNA. Nat Immunol. 2006;7(1):49–56.

33. Means TK, Luster AD. Toll-like receptor activation in the pathogenesis of systemic lupus erythematosus. Ann N Y Acad Sci. 2005;1062:242–51.

34. Ganguly D, Chamilos G, Lande R, Gregorio J, Meller S, Facchinetti V, et al. Self-RNA-antimicrobial peptide complexes activate human dendritic cells through TLR7 and TLR8. J Exp Med. 2009;206(9):1983–94.

35. Wang Y, Swiecki M, McCartney SA, Colonna M. dsRNA sensors and plasmacytoid dendritic cells in host defense and autoimmunity. Immunol Rev. 2011;243(1):74–90.

36. Cervantes-Barragan L, Züst R, Weber F, Spiegel M, Lang KS, Akira S, et al. Control of coronavirus infection through plasmacytoid dendritic-cell-derived type I interferon. Blood. 2007;109(3):1131–7.

37. Döring Y, Manthey HD, Drechsler M, Lievens D, Megens RTA, Soehnlein O, et al. Auto-antigenic protein-DNA complexes stimulate plasmacytoid dendritic cells to promote atherosclerosis. Circulation. 2012;125(13):1673–83.

38. Gregorio J, Meller S, Conrad C, Di Nardo A, Homey B, Lauerma A, et al. Plasmacytoid dendritic cells sense skin injury and promote wound healing through type I interferons. J Exp Med. 2010;207(13):2921–30.

39. Garcia-romo GS, Caielli S, Vega B, Connolly J, Xu Z, Punaro M, et al. Netting Neutrophils Are Major Inducers of Type I IFN Production in Pediatric Systemic Lupus Erythematosus. Sci Transl Med. 2012;3(73).

40. Bave U, Magnusson M, Eloranta M-L, Perers A, Alm G V., Rönnblom L. Fc RIIa Is Expressed on Natural IFN- -Producing Cells (Plasmacytoid Dendritic Cells) and Is Required for the IFN-a Production Induced by Apoptotic Cells Combined with Lupus IgG. J Immunol. 2003;171:3296–302.

41. Tian J, Avalos AM, Mao S-Y, Chen B, Senthil K, Wu H, et al. Toll-like receptor 9-dependent activation by DNA-containing immune complexes is mediated by HMGB1 and RAGE. Nat Immunol. 2007;8(5):487–96.

42. Crow MK, Kirou KA, Wohlgemuth J. Microarray analysis of interferon-regulated genes in SLE. Autoimmunity. 2003;36(8):481–90.

43. Honda K, Vasquez K, Sigrist K, Kucherlapati R, Demant P, Dietrich WF, et al. IRF-7 is the master regulator of type-I interferon-dependent immune responses. Nature. 2005;434(April):772–7.

44. Lande R, Ganguly D, Facchinetti V, Frasca L, Conrad C, Gregorio J, et al. Neutrophils Activate Plasmacytoid Dendritic Cells by Releasing Self-DNA–Peptide Complexes in Systemic Lupus Erythematosus. Sci Transl Med. 2012;3(73):1–20.

45. Campbell AM, Kashgarian M, Shlomchik MJ. NADPH Oxidase Inhibits the Pathogenesis of Systemic Lupus Erythematosus. Sci Transl Med. 2012;4(157):157ra141-157ra141.

46. Di Nuzzo S, Feliciani C, Cortelazzi C, Fabrizi G, Pagliarello C. Immunopathogenesis of Psoriasis: Emphasis on the Role of Th17 Cells. Int Trends Immun. 2014;2(3):3121–2326.

47. Lowes MA, Chamian F, Abello MV, Fuentes-Duculan J, Lin S-L, Nussbaum R, et al. Increase in TNF-alpha and inducible nitric oxide synthase-expressing dendritic cells in psoriasis and reduction with efalizumab (anti-CD11a). Proc Natl Acad Sci USA. 2005;102(52):19057–62.

48. Lande R, Gregorio J, Facchinetti V, Chatterjee B, Wang Y-H, Homey B, et al. Plasmacytoid dendritic cells sense self-DNA coupled with antimicrobial peptide. Nature. 2007;449(7162):564–9.

49. Harder J, Schröder J. Psoriatic scales: a promising source for the isolation of human skin-derived antimicrobial proteins. J Leukoc Biol. 2004;77(4):476–86.

50. Lech M, Gröbmayr R, Weidenbusch M, Anders HJ. Tissues use resident dendritic cells and macrophages to maintain homeostasis and to regain homeostasis upon tissue injury: The immunoregulatory role of changing tissue environments. Mediators Inflamm. 2012;2012.

51. Niessner A, Shin MS, Pryshchep O, Goronzy JJ, Chaikof EL, Weyand CM. Synergistic proinflammatory effects of the antiviral cytokine interferon-α and toll-like receptor 4 ligands in the atherosclerotic plaque. Circulation. 2007;116(18):2043–52.

52. Le Bon A, Schiavoni G, D'Agostino G, Gresser I, Belardelli F, Tough DF. Type I interferons potently enhance humoral immunity and can promote isotype switching by stimulating dendritic cells in vivo. Immunity. 2001;14(4):461–70.

53. Zhang Z, Meng P, Han Y, Shen C, Li B, Hakim MA, et al. Mitochondrial DNA-LL-37 Complex Promotes Atherosclerosis by Escaping from Autophagic Recognition. Immunity. 2015;43(6):1137–47.

54. Caielli S, Athale S, Domic B, Murat E, Chandra M, Banchereau R, et al. Oxidized mitochondrial nucleoids released by neutrophils drive type I interferon production in human lupus. J Exp Med. 2016;jem.20151876.

55. Gary-Gouy H, Lebon P, Dalloul AH. Type I Interferon Production by Plasmacytoid Dendritic Cells and Monocytes Is Triggered by Viruses, but the Level of Production Is Controlled by Distinct Cytokines. J Interf Cytokine Res. 2002;22(6):653–9.

56. Lee EY, Lee CK, Schmidt NW, Jin F, Lande R, Curk T, et al. A review of immune amplification via ligand clustering by self-assembled liquid-crystalline DNA complexes. Adv Colloid Interface Sci. 2016;17-24.

57. Hertzog PJ, Williams BRG. Fine tuning type I interferon responses. Cytokine Growth Factor Rev. 2013;24(3):217–25.

58. Pestka S, Krause CD, Walter MR. Interferons, interferon-like cytokines, and their receptors. Immunol Rev. 2004;202:8–32.

59. Gray P, Goeddel D V. Structure of the human immune interferon gene. Nature. 1982;298:859–63.

60. Lester S, Li K. Toll-like receptors in antiviral innate immunity. J Mol Biol.2014;426(6):1246-64.

61. Pelka K, Latz E. IRF5, IRF8, and IRF7 in human pDCs - the good, the bad, and the insignificant? Eur J Immunol. 2013;43(7):1693–7.

62. Pogue SL, Preston BT, Stalder J, Bebbington CR, Cardarelli PM. The receptor for type I IFNs is highly expressed on peripheral blood B cells and monocytes and mediates a distinct profile of differentiation and activation of these cells. J Interferon Cytokine Res. 2004;24(2):131–9.

63. Roisman LC, Jaitin DA, Baker DP, Schreiber G. Mutational analysis of the IFNAR1 binding site on IFN-α2 reveals the architecture of a weak ligand-receptor binding-site. J Mol Biol. 2005;353(2):271–81.

64. Piehler J, Roisman LC, Schreiber G. New structural and functional aspects of the type I interferon-receptor interaction revealed by comprehensive mutational analysis of the binding interface. J Biol Chem. 2000;275(51):40425–33.

65. Cao W, Bover L, Cho M, Wen X, Hanabuchi S, Bao M, et al. Regulation of TLR7/9 responses in plasmacytoid dendritic cells by BST2 and ILT7 receptor interaction. J Exp Med. 2009;206(7):1603–14.

66. Prakash A, Smith E, Lee CK, Levy DE. Tissue-specific positive feedback requirements for production of type I interferon following virus infection. J Biol Chem. 2005;280(19):18651–7.

67. Le Bon A, Etchart N, Rossmann C, Ashton M, Hou S, Gewert D, et al. Cross-priming of CD8+ T cells stimulated by virus-induced type I interferon. Nat Immunol. 2003;4(10):1009–15.

68. Mescher MF, Curtsinger JM, Agarwal P, Casey KA, Gerner M, Hammerbeck CD, et al. Signals required for programming effector and memory development by CD8+ T cells. Immunol Rev. 2006;211:81–92.

69. Krug A, Uppaluri R, Facchetti F, Dorner BG, Sheehan KCF, Schreiber RD, et al. IFN-producing cells respond to CXCR3 ligands in the presence of CXCL12 and secrete inflammatory chemokines upon activation. J Immunol. 2002;169(11):6079–83.

70. Lin X, Kong J, Wu Q, Yang Y, Ji P. Effect of TLR4/MyD88 signaling pathway on expression of IL-1β and TNF-α in synovial fibroblasts from temporomandibular joint exposed to lipopolysaccharide. Mediators Inflamm. 2015;2015.

71. Guo YJ, Luo T, Wu F, Mei YW, Peng J, Liu H, et al. Involvement of TLR2 and TLR9 in the anti-inflammatory effects of chlorogenic acid in HSV-1-infected microglia. Life Sci. 2015;127:12–8.

72. Blank SE, Johnson EC, Weeks DK, Wysham CH. Circulating dendritic cell number and intracellular TNF-α production in women with type 2 diabetes. Acta Diabetol. 2012;49(1 Suppl 1.):25–32.

73. Steinhagen F, Meyer C, Tross D, Gursel M, Maeda T, Klaschik S, et al. Activation of type I interferon-dependent genes characterizes the “core response” induced by CpG DNA. J Leukoc Biol. 2012;92:775–85.

74. Hurst J, Prinz N, Lorenz M, Bauer S, Chapman J, Lackner KJ, et al. TLR7 and TLR8 ligands and antiphospholipid antibodies show synergistic effects on the induction of IL-1β and caspase-1 in monocytes and dendritic cells. Immunobiology. 2009;214(8):683–91.

75. Elssner A, Duncan M, Gavrilin M, Wewers MD. A Novel P2X7 Receptor Activator, the Human Cathelicidin-Derived Peptide LL37, Induces IL-1 Processing and Release. J Immunol. 2004;172(8):4987–94.

76. Dombrowski Y, Schauber J. Cathelicidin LL-37: A defense molecule with a potential role in psoriasis pathogenesis. Exp Dermatol. 2012;21(5):327–30.

77. Sorrentino R, Terlizzi M, Di Crescenzo VG, Popolo A, Pecoraro M, Perillo G, et al. Human lung cancer-derived immunosuppressive plasmacytoid dendritic cells release IL-1α in an AIM2 inflammasome-dependent manner. Am J Pathol. 2015;185(11):3115–24.

78. Anand PK, Malireddi RKS, Kanneganti TD. Role of the Nlrp3 inflammasome in microbial infection. Front Microbiol. 2011;2(FEB):1–6.

79. Johansen C, Moeller K, Kragballe K, Iversen L. The Activity of Caspase-1 Is Increased in Lesional Psoriatic Epidermis. J Invest Dermatol. 2007;127(12):2857–64.

80. Guiducci C, Tripodo C, Gong M, Sangaletti S, Colombo MP, Coffman RL, et al. Autoimmune skin inflammation is dependent on plasmacytoid dendritic cell activation by nucleic acids via TLR7 and TLR9. 2010;207(13).

81. Lozza L, Farinacci M, Faé K, Bechtle M, Stäber M, Dorhoi A, et al. Crosstalk between human DC subsets promotes antibacterial activity and CD8+ T-cell stimulation in response to bacille Calmette-Guérin. Eur J Immunol. 2014;44(1):80–92.

82. Barchet W, Cella M, Odermatt B, Asselin-Paturel C, Colonna M, Kalinke U. Virus-induced interferon alpha production by a dendritic cell subset in the absence of feedback signaling in vivo. J Exp Med. 2002;195(4):507–16.

83. Ewald SE, Lee BL, Lau L, Wickliffe KE, Shi G-P, Chapman HA, et al. The ectodomain of Toll-like receptor 9 is cleaved to generate a functional receptor. Nature. 2008;456(7222):658–62.

84. Honda K, Ohba Y, Hideyuki H, Negishi T, Mizutani A, Takaoka C, et al. Spatiotemporal regulation of MyD88 – IRF-7 signalling for robust type-I interferon induction Page 1 of 6. Nature. 2005;434(0):1–6.

85. Ewald SE, Engel A, Lee J, Wang M, Bogyo M, Barton GM. Nucleic acid recognition by Toll-like

receptors is coupled to stepwise processing by cathepsins and asparagine endopeptidase. J Exp Med. 2011;208(4):643–51.

86. Burns K, Clatworthy J, Martin L, Martinon F, Plumpton C, Maschera B, et al. Tollip, a new component of the IL-1RI pathway, links IRAK to the IL-1 receptor. Nat Cell Biol. 2000;2(6):346–51.

87. Ito T, Kanzler H, Duramad O, Cao W, Liu YJ. Specialization, kinetics, and repertoire of type 1 interferon responses by human plasmacytoid predendritic cells. Blood. 2006;107(6):2423–31.

88. Honda K, Takaoka A, Taniguchi T. Type I Inteferon Gene Induction by the Interferon Regulatory Factor Family of Transcription Factors. Immunity. 2006;25(3):349–60.

89. Sasai M, Linehan MM, Iwasaki A. Bifurcation of Toll-Like Receptor 9 Signaling by Adaptor Protein 3. Science (80-). 2010;329(5998):1530–4.

90. Henault J, Martinez J, Riggs JM, Tian J, Mehta P, Clarke L, et al. Noncanonical Autophagy Is Required for Type I Interferon Secretion in Response to DNA-Immune Complexes. Immunity. 2012;37(6):986–97.

91. Yang K, Puel A, Zhang S, Eidenschenk C, Ku CL, Casrouge A, et al. Human TLR-7-, -8-, and -9-mediated induction of IFN-α/β and -λ Is IRAK-4 dependent and redundant for protective immunity to viruses. Immunity. 2005;23(5):465–78.

92. Kawai T, Sato S, Ishii KJ, Coban C, Hemmi H, Yamamoto M, et al. Interferon-α induction through Toll-like receptors involves a direct interaction of IRF7 with MyD88 and TRAF6. Nat Immunol. 2004;5(10):1061–8.

93. Honda K, Yanai H, Mizutani T, Negishi H, Shimada N, Suzuki N, et al. Role of a transductional-transcriptional processor complex involving MyD88 and IRF-7 in Toll-like receptor signaling. Proc Natl Acad Sci USA. 2004;101(43):15416–21.

94. Shinohara ML, Lu L, Bu J, Werneck MBF, Kobayashi KS, Glimcher LH, et al. Osteopontin expression is essential for interferon-α production by plasmacytoid dendritic cells. Nat Immunol. 2006;7(5):498–506.

95. Deng L, Wang C, Spencer E, Yang L, Braun A, You J, et al. Activation of the IκB Kinase Complex by TRAF6 Requires a Dimeric Ubiquitin-Conjugating Enzyme Complex and a Unique Polyubiquitin Chain. Cell. 2000;103(2):351–61.

96. Wang C, Deng L, Hong M, Akkaraju GR, Inoue J, Chen ZJ. TAK1 is a ubiquitin-dependent kinase of MKK and IKK. Nature. 2001;412(6844):346–51.

97. Osawa Y, Iho S, Takauji R, Takatsuka H, Yamamoto S, Takahashi T, et al. Collaborative action of NF-kappaB and p38 MAPK is involved in CpG DNA-induced IFN-alpha and chemokine production in human plasmacytoid dendritic cells. J Immunol. 2006;177(7):4841–52.

98. Kerkmann M, Costa LT, Richter C, Rothenfusser S, Battiany J, Hornung V, et al. Spontaneous formation of nucleic acid-based nanoparticles is responsible for high interferon-α induction by CpG-A in plasmacytoid dendritic cells. J Biol Chem. 2005;280(9):8086–93.

99. Hartmann G, Weeratna RD, Ballas ZK, Payette P, Blackwell S, Suparto I, et al. Delineation of a CpG Phosphorothioate Oligodeoxynucleotide for Activating Primate Immune Responses In Vitro and In Vivo. J Immunol. 2000;164(3):1617–24.

100. Coch C, Busch N, Wimmenauer V, Hartmann E, Janke M, Abdel-Mottaleb MMA, et al. Higher activation of TLR9 in plasmacytoid dendritic cells by microbial DNA compared with self-DNA based on CpG-specific recognition of phosphodiester DNA. J Leukoc Biol. 2009;86(3):663–70.

101. Verthelyi D, Ishii KJ, Gursel M, Takeshita F, Klinman DM. Human Peripheral Blood Cells Differentially Recognize and Respond to Two Distinct CpG Motifs. J Immunol. 2001;166(4):2372–7.

102. Latz E, Schoenemeyer A, Visintin A, Fitzgerald KA, Monks BG, Knetter CF, et al. TLR9 signals after translocating from the ER to CpG DNA in the lysosome. Nat Immunol. 2004;5(2):190–8.

103. Kim T, Pazhoor S, Bao M, Zhang Z, Hanabuchi S, Facchinetti V, et al. Aspartate-glutamate-alanine-histidine box motif (DEAH)/RNA helicase A helicases sense microbial DNA in human plasmacytoid dendritic cells. Proc Natl Acad Sci. 2010;107(34):15181–6.

104. Kumagai Y, Kumar H, Koyama S, Kawai T, Takeuchi O, Akira S. Cutting Edge: TLR-Dependent Viral Recognition Along with Type I IFN Positive Feedback Signaling Masks the Requirement of Viral Replication for IFN- Production in Plasmacytoid Dendritic Cells. J Immunol.

2009;182(7):3960–4.

105. Svensson D, Wilk L, Mörgelin M, Herwald H, Nilsson B-O. LL-37-induced host cell cytotoxicity depends on cellular expression of the globular C1q receptor (p33). Biochem J. 2016;473(1):87–98.

106. Zasloff M. Antimicrobial peptides of multicellular organisms. Nature. 2002;415(0028–0836):389–95.

107. Oppenheim JJ, Yang D. Alarmins: Chemotactic activators of immune responses. Curr Opin Immunol. 2005;17(4 SPEC. ISS.):359–65.

108. Zhang Z, Cherryholmes G, Shively JE. Neutrophil secondary necrosis is induced by LL-37 derived from cathelicidin. J Leukoc Biol. 2008;84(3):780–8.

109. Sandgren S, Wittrup A, Cheng F, Jönsson M, Eklund E, Busch S, et al. The Human Antimicrobial Peptide LL-37 Transfers Extracellular DNA Plasmid to the Nuclear Compartment of Mammalian Cells via Lipid Rafts and Proteoglycan-dependent Endocytosis. J Biol Chem. 2004;279(17):17951–6.

110. Dürr UHN, Sudheendra US, Ramamoorthy A. LL-37, the only human member of the cathelicidin family of antimicrobial peptides. Biochim Biophys Acta - Biomembr. 2006;1758(9):1408–25.

111. Zhang X, Oglęcka K, Sandgren S, Belting M, Esbjörner EK, Nordén B, et al. Dual functions of the human antimicrobial peptide LL-37-Target membrane perturbation and host cell cargo delivery. Biochim Biophys Acta - Biomembr. 2010;1798(12):2201–8.

112. Pinegin B V, Pashenkov M V, Kulakov V V, Murugin V V, Zhmak MN. Complexes of DNA with the Antimicrobial Peptide LL37 Augment NK Cell Functions by Inducing. 2015;35(11):850–8.

113. Lande R, Chamilos G, Ganguly D, Demaria O, Frasca L, Durr S, et al. Cationic antimicrobial peptides in psoriatic skin cooperate to break innate tolerance to self-DNA. Eur J Immunol. 2015;45(1):203–13.

114. Scaffidi P, Misteli T, Bianchi ME. Release of chromatin protein HMGB1 by necrotic cells triggers inflammation. Nature. 2010;467(7315):622–622.

115. Elkon KB, Santer DM. Complement, interferon and lupus. Curr Opin Immunol. 2012;24(6):665–70.

116. Muruve DA, Pétrilli V, Zaiss AK, White LR, Clark SA, Ross PJ, et al. The inflammasome recognizes cytosolic microbial and host DNA and triggers an innate immune response. Nature. 2008;452(7183):103–7.

117. Pazmandi K, Agod Z, Kumar B V., Szabo A, Fekete T, Sogor V, et al. Oxidative modification enhances the immunostimulatory effects of extracellular mitochondrial DNA on plasmacytoid dendritic cells. Free Radic Biol Med. 2014;77:281–90.

118. Maeda T, Murata K, Fukushima T, Sugahara K, Tsuruda K, Anami M, et al. A novel plasmacytoid dendritic cell line, CAL-1, established from a patient with blastic natural killer cell lymphoma. Int J Hematol. 2005;81(2):148–54.

119. Hilbert T, Steinhagen F, Weisheit C, Baumgarten G, Hoeft A, Klaschik S. Synergistic stimulation with different TLR7 ligands modulates gene expression patterns in the human plasmacytoid dendritic cell line CAL-1. Mediators Inflamm. 2015;2015.

120. Steinhagen F, Mcfarland AP, Rodriguez LG, Tewary P, Jarret A, Savan R, et al. IRF-5 and NF-κB p50 co-regulate IFN-β and IL-6 expression in TLR9-stimulated human plasmacytoid dendritic cells. Eur J Immunol. 2013;43(7):1896–906.

121. Rocha H, Ferreira R, Carvalho J, Vitorino R, Santa C, Lopes L, et al. Characterization of mitochondrial proteome in a severe case of ETF-QO deficiency. J Proteomics. 2011;75(1):221–8.

122. Combes A, Camosseto V, N'Guessan P, Argüello RJ, Mussard J, Caux C, et al. BAD-LAMP controls TLR9 trafficking and signalling in human plasmacytoid dendritic cells. Nat Commun. 2017;8(1):913.